Nucleon Elastic Form Factors
Past, Present & Future

Donal Day
University of Virginia

HUGS, June 2007

Outline

- Introduction, Motivation and Formalism
- Traditional Techniques and Data
- Models
- New Data
  - Recoil Polarization
  - Beam-Target Asymmetry
  - Ratio method
- Rosenbluth-Polarization Discrepancy and Two-Photon Corrections
- Prospects and Summary

Nucleons have Structure and Size!

Early Indications

- ✳ Anomalous magnetic moments of p and n
  O. Stern, Nature 132 (1933) 169
- ✳ Non-zero neutron charge radius from scattering of thermal neutrons on atoms
- ✓ The deviation of experimental data from curve (c) was interpreted as an effect from proton form factors - finite size proton.
  $\langle r_E^2 \rangle^{1/2}_{(\text{proton})} =$
  $\langle r_M^2 \rangle^{1/2}_{(\text{proton})} = 0.86$ fm.

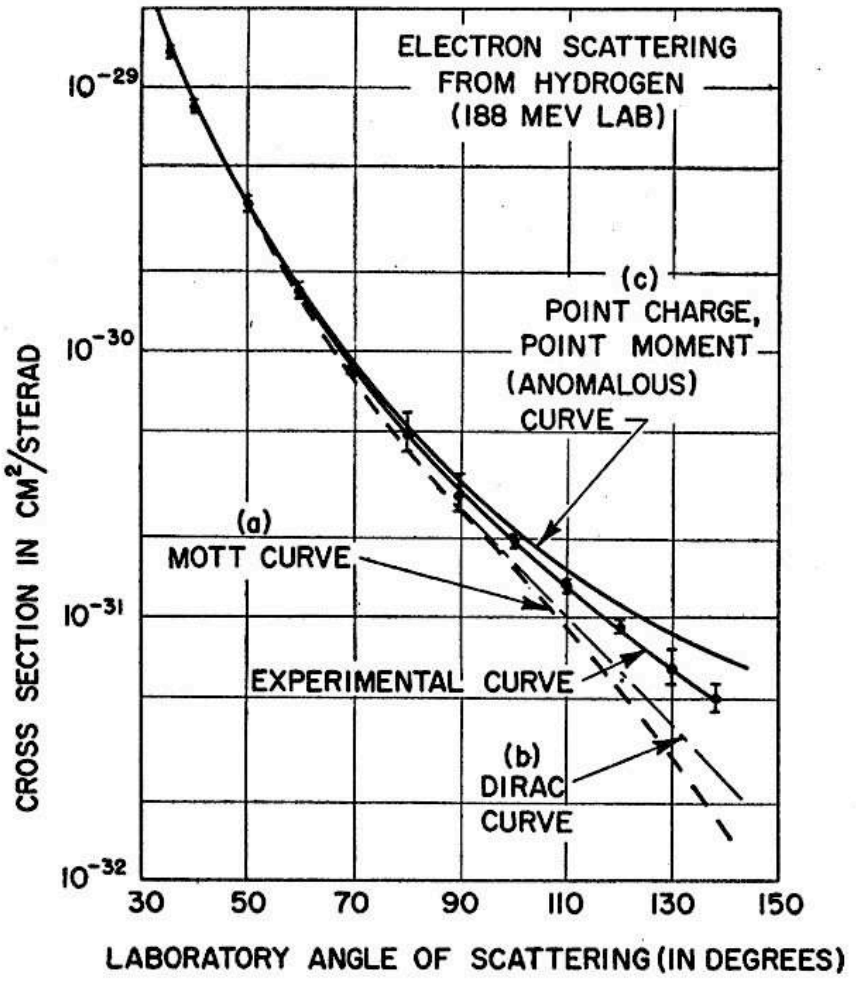

Hofstader and McAllister, 1956

Motivation

- FF are fundamental quantities
- Describe the internal structure of the nucleon
- Provide rigorous tests of QCD description of the nucleon
- Necessary for study of nuclear structure

  Few body structure functions

  Important input to Parity violating experiments

50 years of effort $\cdots$ what is new?

- New techniques, unexpected behavior, and a reinvigorated theoretical effort have made the last decade one of important progress.

Formalism

$$\frac{d\sigma}{d\Omega} = \sigma_{\rm Mott}\frac{E'}{E_0}\left\{(F_1)^2 + \tau\left[2\left(F_1+F_2\right)^2\tan^2\left(\theta_e\right) + \left(F_2\right)^2\right]\right\}; F_{1,2} = F_{1,2}(Q^2)$$

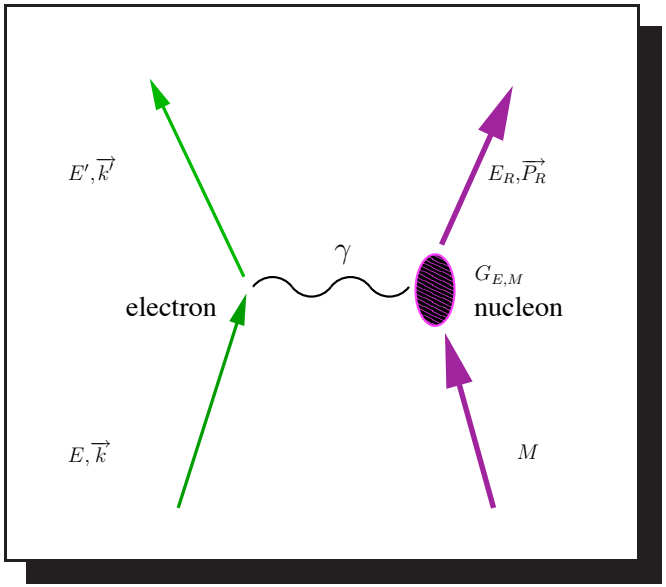

$Q^2 = 4EE'\sin^2(\theta/2)$	$\tau = \frac{Q^2}{4M^2}$
$F_1^p(0) = 1$	$F_1^n(0) = 0$
$F_2^p(0) = 1.79$	$F_2^n(0) = -1.91$

In Breit frame F_1 and F_2 related to charge and spatial curent densities:

$$\rho = J_0 = 2eM[F_1 - \tau F_2]$$

$$J_i = e\bar{u}\gamma_i u[F_1 + F_2]_{i=1,2,3}$$

$$G_E\left(Q^2\right) = F_1(Q^2) - \tau F_2\left(Q^2\right) \qquad G_M\left(Q^2\right) = F_1\left(Q^2\right) + F_2\left(Q^2\right)$$

✓ For a point like probe G_E and G_M are the FT of the charge and magnetizations distributions in the nucleon, with the following normalizations

$Q^2 = 0$ limit: $G_E^p = 1$ $G_E^n = 0$ $G_M^p = 2.79$ $G_M^n = -1.91$

one-photon approx.

Form Factors

➙ First introduced to describe the scattering on an extended charge distribution, $\rho(r)$, such that $\int \rho(r) d^3r = 1$

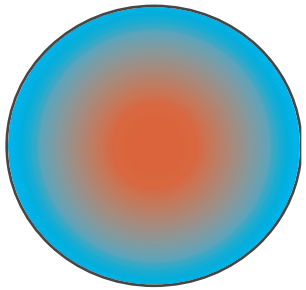

We define the form factor as the Fourier transform of the spatial distribution function,

$$F(q) = \int e^{iqr} \rho(r) d^3r$$

Charge distribution		Form Factor	
point	$\rho(r) = \delta(r - r_o)$	$F(q^2) = 1$	unity
exponential	$\rho(r) = \frac{a^3}{8\pi} e^{-ar}$	$F(q^2) = \left[\frac{1}{1+q^2/a^2}\right]^2$	dipole
Yukawa	$\rho(r) = \frac{a^2}{4\pi r} e^{-ar}$	$F(q^2) = \frac{1}{1+q^2/a^2}$	pole
Gaussian	$\rho(r) = \left(\frac{a^2}{2\pi}\right)^{3/2} e^{-(a^2 r^2/2)}$	$F(q^2) = e^{-(q^2/2a^2)}$	Gaussian

Form factor modifies the cross section formula in a simple way:

$$\frac{d\sigma}{d\Omega} \Rightarrow \frac{d\sigma}{d\Omega} \mid F(q^2) \mid^2$$

Rosenbluth formula, separation

$$\frac{d\sigma}{d\Omega} = \sigma_{\rm NS}\left[\frac{G_E^2+\tau G_M^2}{1+\tau} + 2\tau G_M^2 \tan^2(\theta/2)\right]$$

$$\sigma_R \equiv \frac{d\sigma}{d\Omega}\frac{\epsilon(1+\tau)}{\sigma_{\rm NS}} = \underbrace{\tau G_M^2(Q^2)}_{\text{intercept}} + \epsilon \underbrace{G_E^2(Q^2)}_{\text{slope}}$$

① Intercept and slope give G_M and G_E

② G_M dominates for large τ.

③ Must control kinematics, acceptances and radiative corrections.

④ Data consistent with one-photon exchange

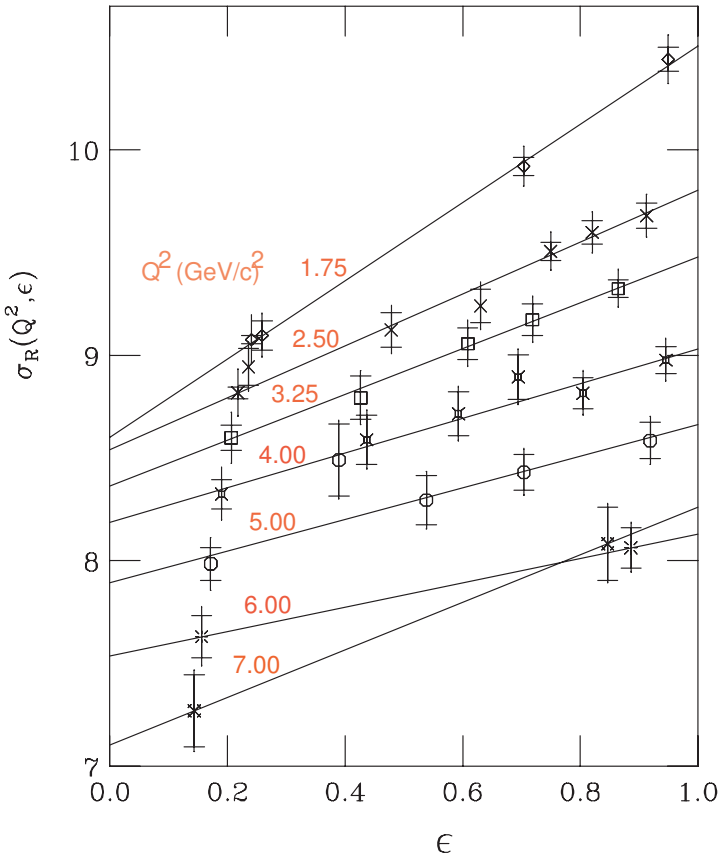

SLAC, Andivahis, Bosted *et al.*

$$\tau = \frac{Q^2}{4M^2} \quad \epsilon^{-1} = 1 + 2(1+\tau)\tan(\theta/2)^2$$

Proton data from Rosenbluth

$$\underbrace{G_E^p(Q^2) \approx \frac{G_M^p(Q^2)}{\mu_p} \approx \frac{G_M^n(Q^2)}{\mu_n}}_{\text{Scaling Law}} \approx \underbrace{G_D \equiv \left(1 + \frac{Q^2}{0.71}\right)^{-2}}_{\text{Dipole Law}}$$

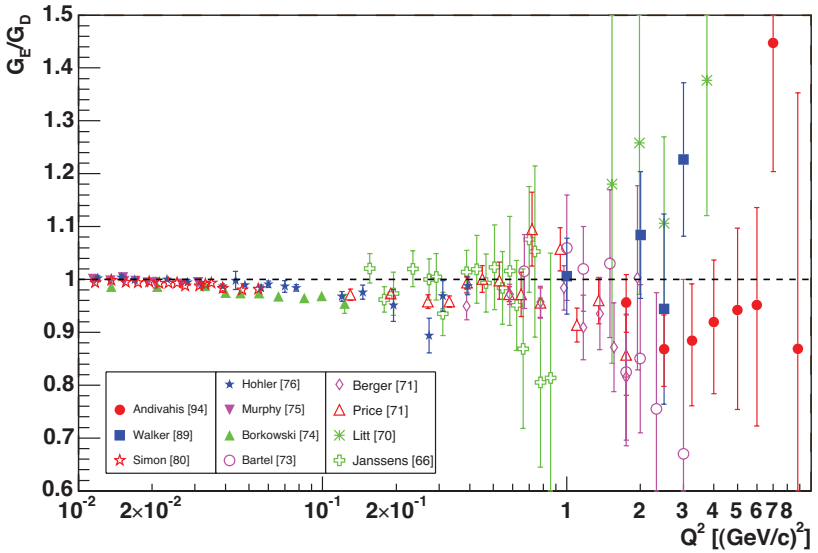

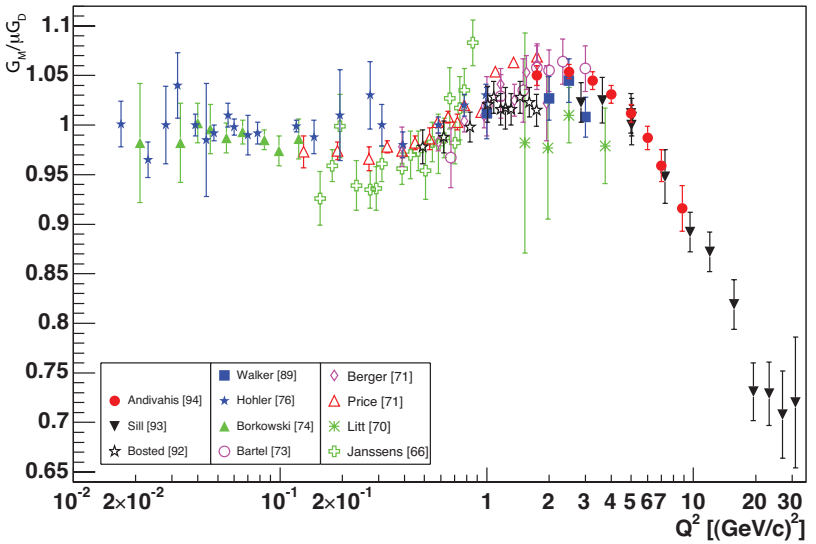

- ✓ G_E^p consistent with G_D, but large uncertainties at large Q^2 and systematic differences foreshadow limitations of Rosenbluth
- ✓ G_M^p modified relative to G_D at large Q^2

Neutron Form Factor Measurements

- No neutron target
- proton dominates neutron
- G_M^n dominates G_E^n

G_M^n and G_E^n have been measured through:

① Elastic scattering $^2\mathrm{H}(e,e')^2\mathrm{H}$

② Inclusive quasielastic scattering: $^2\mathrm{H}(e,e')X$

③ Exclusive quasielastic: neutron in coincidence: $^2\mathrm{H}(e,e'n)p$

④ Ratio techniques $\frac{d(e,e'n)p}{d(e,e'p)n}$ (quasielastic)

Complications: Rosenbluth, subtraction of proton

Even with simplest nucleus – no escaping nuclear physics

G_M^n unpolarized

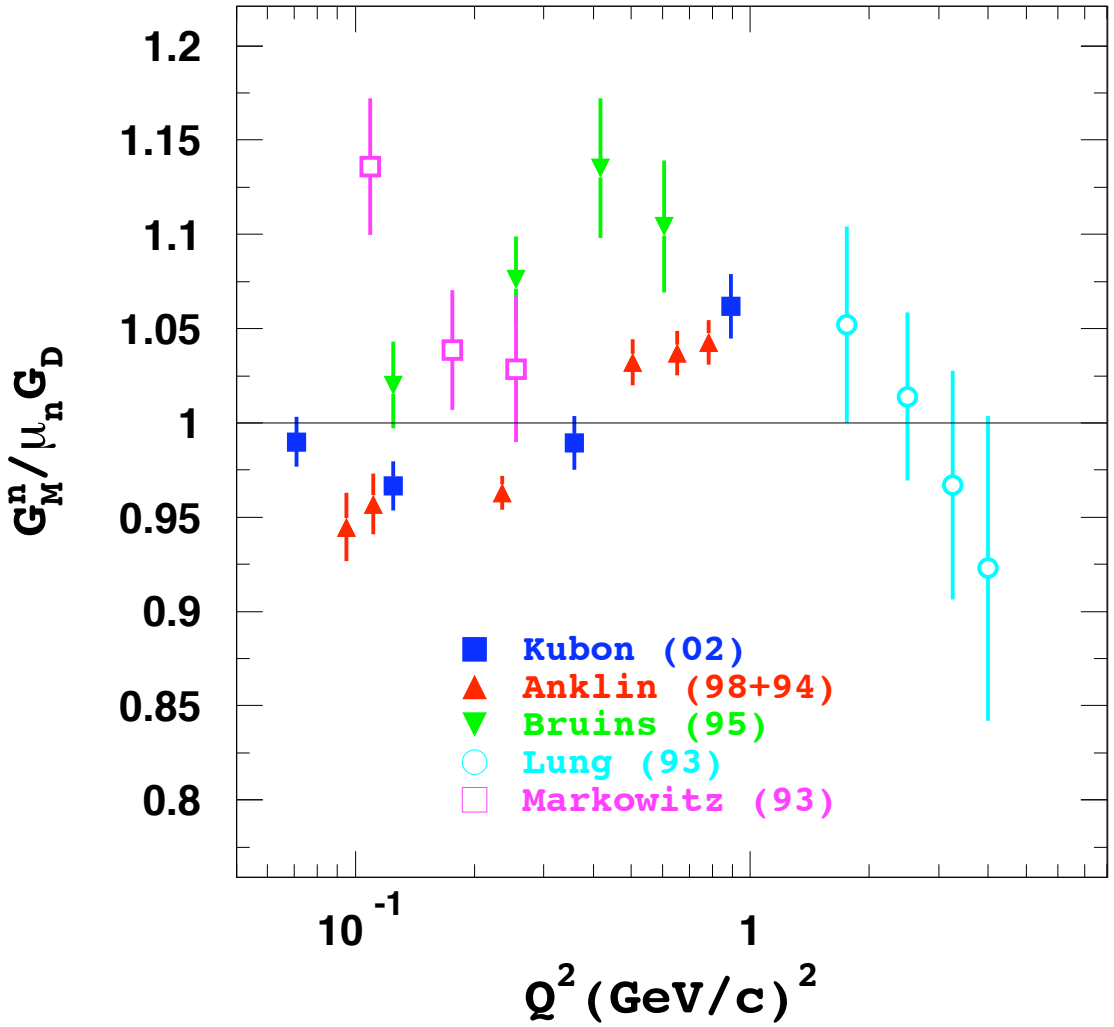

Kubon	ratio
Anklin	ratio
Bruins	ratio
Lung	$D(e,e')X$
Markowitz	$D(e,e'n)p$

$$\text{ratio} \equiv \frac{D(e,e'n)p}{D(e,e'p)n}$$

neutron detection efficiency!!

G_E^n from e-D elastic scattering

In IA elastic e-D is sum of proton and neutron responses with deuteron wf weighting and in small θ_e approximation

$$\frac{d\sigma}{d\Omega} \simeq \sigma_{\rm Mott}(G_E^p + G_E^n)^2 \left[u(r)^2 + w(r)^2\right] j_0(\frac{qr}{2})dr \cdots$$

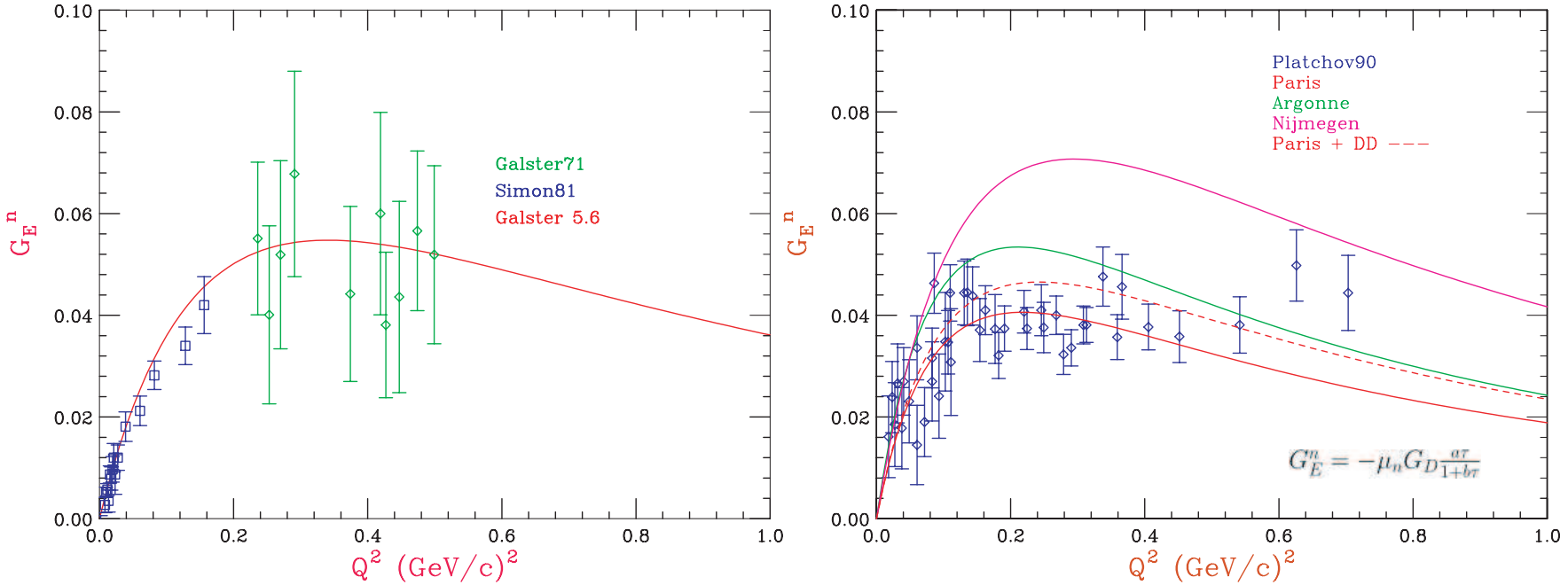

Galster Parametrization: $G_E^n = -\frac{\tau\mu_n}{1+5.6\tau}G_D$

70's, 80's, & 90's

Models of Nucleon Form Factors

Dispersion relations

Formalism is model independent

$$F(t) = \frac{1}{\pi}\int_{t_0} \frac{\mathrm{Im}F(t')}{t'-t}dt'$$

Hoehler (1976), Hammer, Mergell, Meissner, Drechsel. Imaginary part of the spectral function receive contributions from all the possible intermediate states. Modeling is still necessary.

VMD

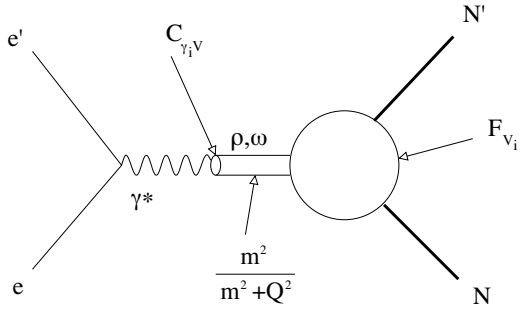

$$F(Q^2) = \sum_i \frac{C_{\gamma V_i}}{Q^2+M^2_{V_i}} F_{V_i N}(Q^2)$$

IJL,Gari, Krumpelmann
Spectral function is approximated by a series of poles corresponding to vector mesons, ω, ϕ, and ρ appearing along the real axis. Fails to reproduce the large Q^2 behavior of pQCD.

---

pQCD

$$F_2 \propto F_1\left(\frac{M}{Q^2}\right)$$

$$F_1 \propto \frac{\alpha_s^2(Q^2)}{Q^4}$$

$$Q^2\frac{F_2}{F_1} \rightarrow \text{constant}$$

Farrar&Jackson, Brodksy&Lepage
Helicity conservation
Counting rules

JLAB data: $Q\frac{F_2}{F_1} \rightarrow$ constant

Models of Nucleon Form Factors

VMD-pQCD	At low Q^2 $F_1 \sim F_2 \sim \frac{\Lambda_1^2}{\Lambda_1^2+Q^2}$ with $\Lambda_1 \sim 0.8$ GeV At large Q^2 $F_1 \sim \left[\frac{1}{Q^2 \log(Q^2/\Lambda^2_{\rm QCD})}\right]$ $F_2 \sim \frac{F_1}{Q^2}$	Gari & Krumpelmann, Lomon, Bijker Failure to follow the high Q^2 behavior suggested by pQCD led GK to incorporate pQCD at high Q^2 with the low VMD behavior. Inclusion of ϕ by GK had significant effect on G_E^n. Lomon has updated with new fits to selected data.
Lattice	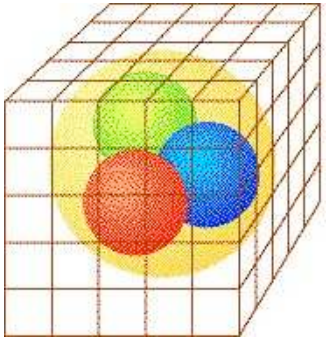	Draper, Liu, .. Dong, Liu, &Williams; Thomas, QCDSF Limitations in computer speed; quark masses 5-10 times higher than the physical values; quenched QCD, extrapolations are varied
RCQM	light front point form	Miller.., Cardarelli & Simula CM motion and relative motion of quarks separated, SU(6) symmetry breaking by Melosh rotations Wagenbrunn... PFSA, GBE

Models of Nucleon Form Factors

CBM	$\mathcal{L}_{\rm CBM} \cong \mathcal{L}_{\rm MITBag} + \mathcal{L}_{\rm Free-\pi} + \mathcal{L}_{\rm int}$	Lu, Thomas, Williams
LFCBM	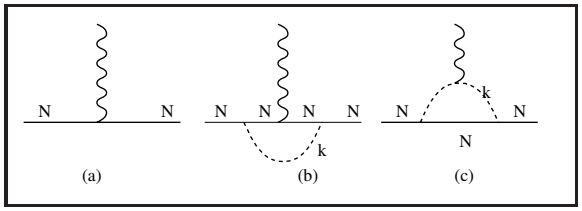	Miller pion cloud
Helicity	Helicity non-conservation through Quark orbital angular momentum	Ralston.. (pQCD) Miller...(RCQM) Brodsky

Data and Theory, Proton

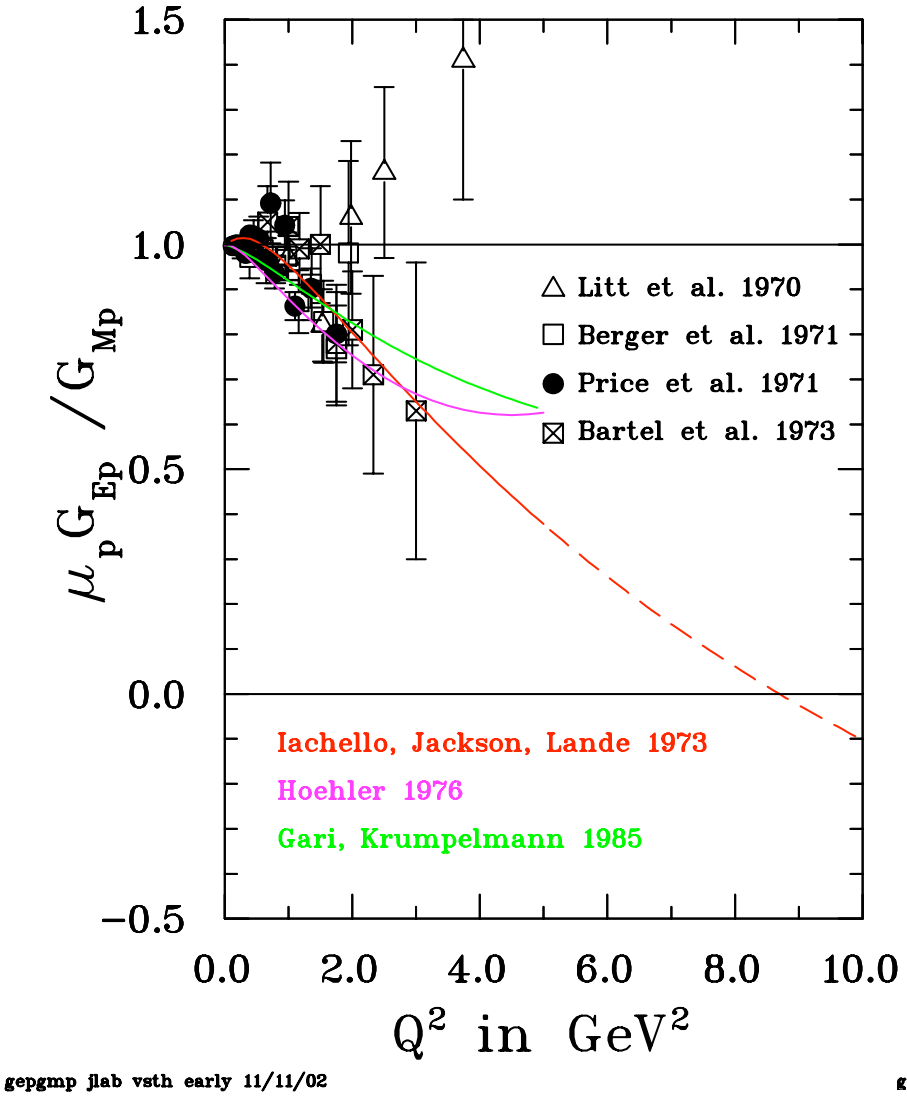

Data and Theory (1980's)

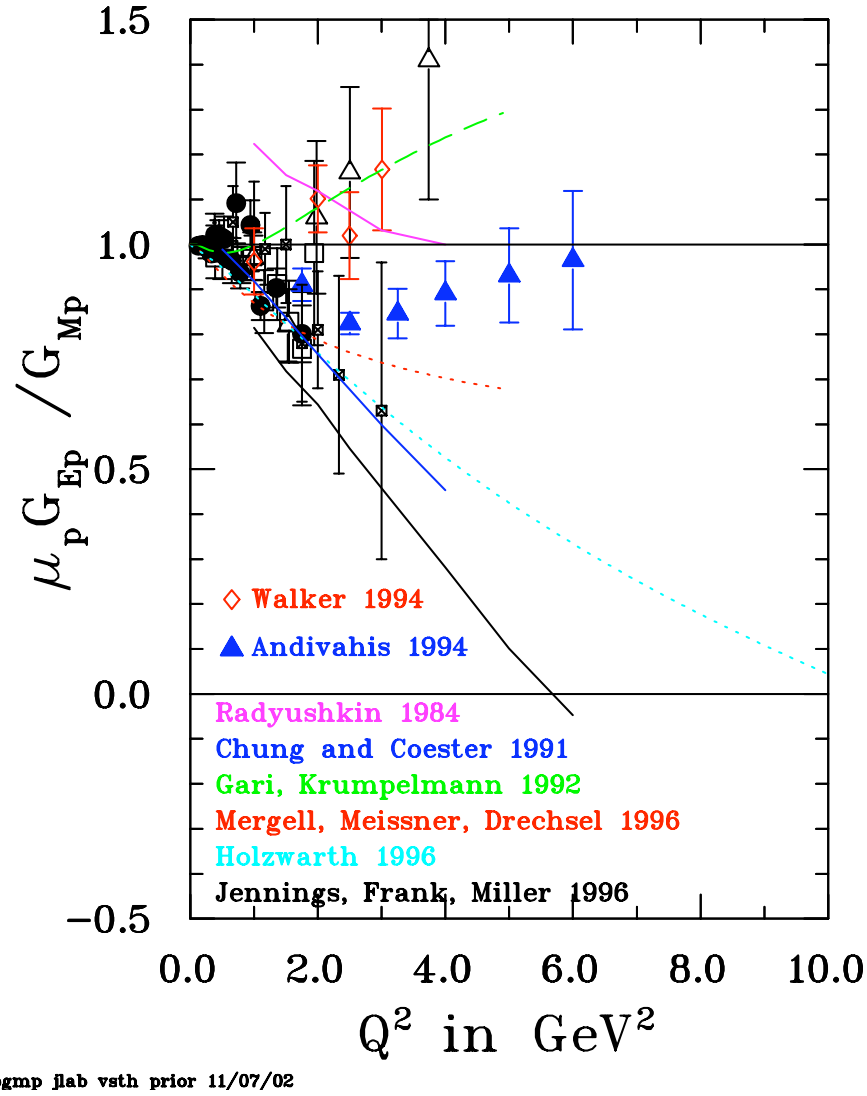

Data and Theory (1990's)

Data and Theory, G_E^n

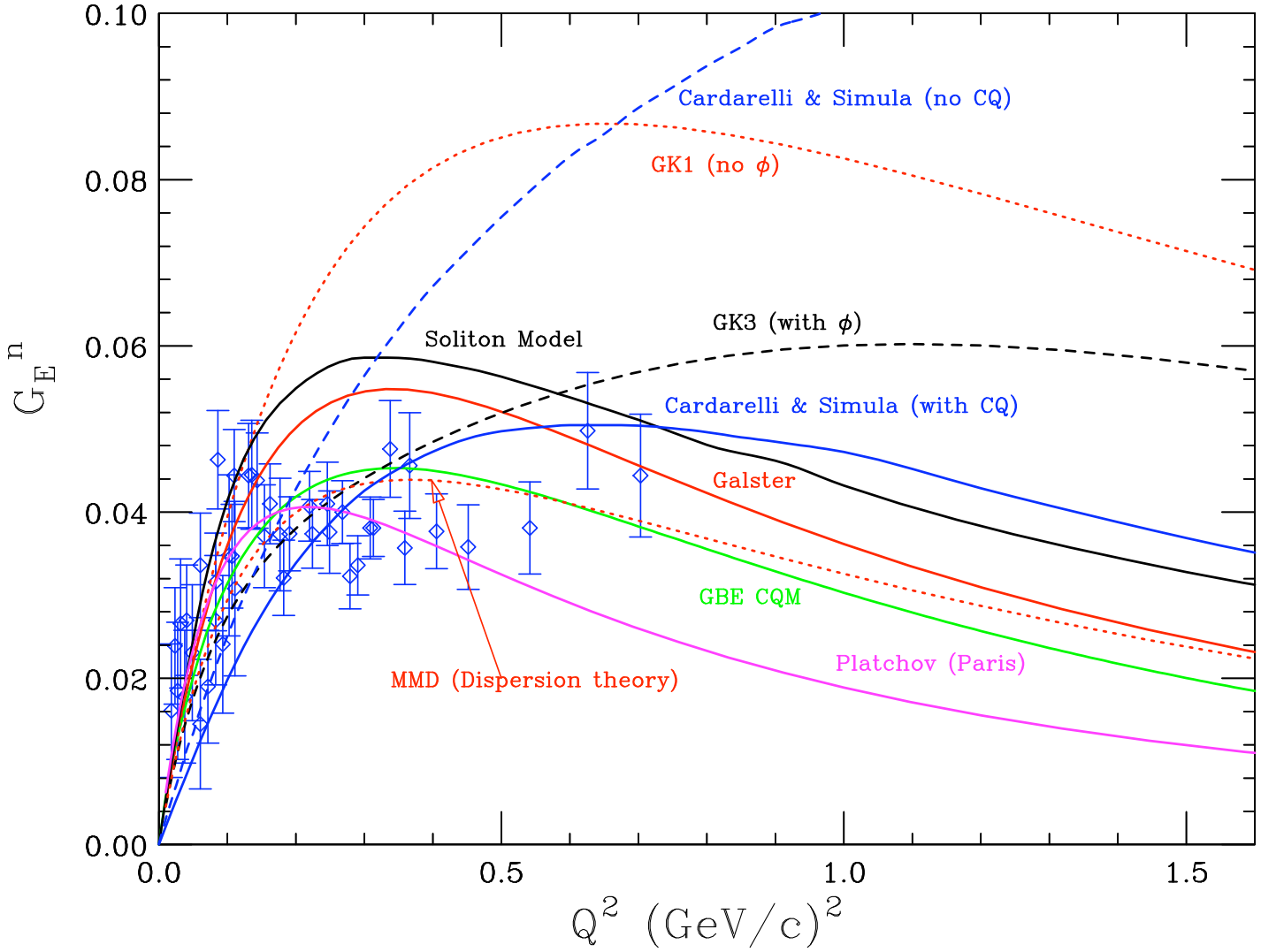

How to measure small quantities like G_E^n (or G_E^p)?

Use spin observables since they often result from interference between amplitudes

Very Schematically

some operator $\mathcal{O} = \mathcal{O}_{\rm Big} + \mathcal{O}_{\rm Small}$

unpolarized crossection: $d\sigma \propto \ |\langle f \mid \mathcal{O}_{\rm Big} \mid i\rangle|^2 + |\langle f \mid \mathcal{O}_{\rm Small} \mid i\rangle|^2$

while spin observables contain terms like: $\langle f \mid \mathcal{O}_{\rm Big} \mid i\rangle^\star \langle f \mid \mathcal{O}_{\rm Small} \mid i\rangle$

which is linear in small quantity but with a large coefficient.

For the form factors : $\mathcal{O} \propto G_E G_M$ instead of $\mathcal{O} \propto G_E^2 + G_M^2$

Two techniques

- ✷ Recoil Polarization
- ✷ Beam-Target Asymmetry

Spin Correlations in elastic scattering

Essential feature:

$$\frac{d\sigma}{d\Omega} = \underbrace{\ldots (G_E^2 + \ldots G_M^2)}_{(d\sigma/d\Omega)_{\rm unpol}} + \underbrace{\ldots P_e P_N^{\perp} G_E G_M}_{A_T} + \underbrace{\ldots P_e P_N^{\parallel} G_M^2}_{A_\parallel}$$

First work at Bates and Mainz starting in early 1990's

- ✳ Dombey, Rev. Mod. Phys. **41** 236 (1968): $\vec{p}(\vec{e}, e')$
- ✳ Akheizer and Rekalo, Sov. Phys. Doklady **13** 572 (1968): $p(\vec{e}, e', \vec{p})$
- ✳ Arnold, Carlson and Gross, Phys. Rev. C **23** 363 (1981): $^2\mathrm{H}(\vec{e}, e'\vec{n})p$
- ✳ Blankleider and Woloshyn, Phys. Rev. C **29**, 538 (1984)

  polarized ^{3}He as an effective polarized neutron target

Recoil Polarization

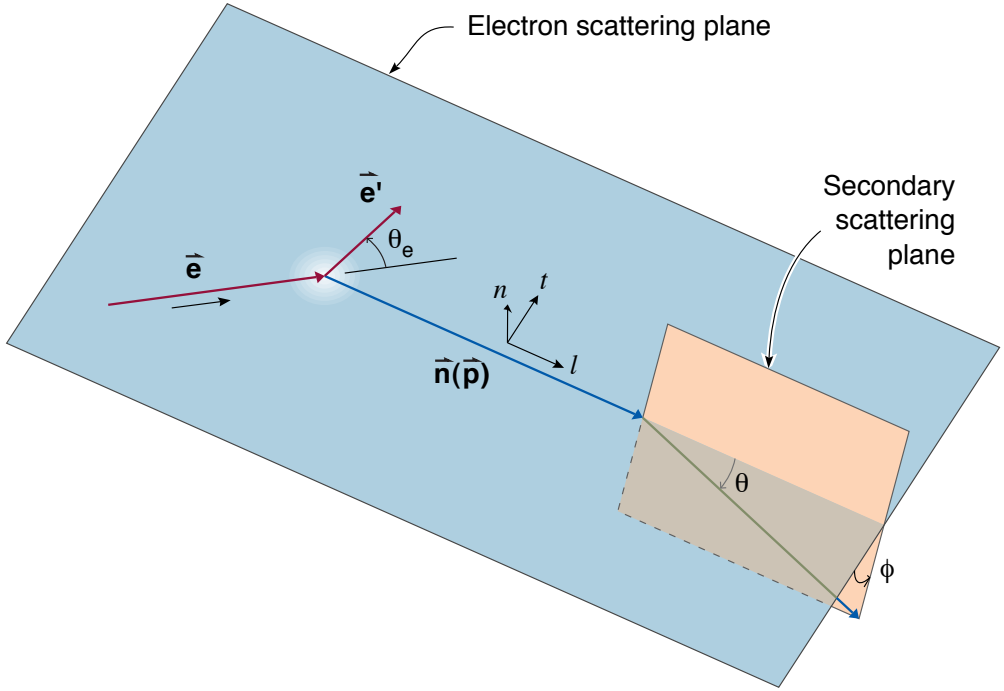

$$I_0 P_t = -2\sqrt{\tau(1+\tau)}\, G_E G_M \tan(\theta_e/2)$$

$$I_0 P_l = \frac{1}{M_N}(E_e + E_{e'})\sqrt{\tau(1+\tau)}\, G_M^2 \tan^2(\theta_e/2)$$

$$\frac{G_E}{G_M} = -\frac{P_t}{P_l}\frac{(E_e+E_{e'})}{2M_N}\tan\left(\frac{\theta_e}{2}\right)$$

Direct measurement of form factor ratio by measuring the ratio of the transfered polarization P_t and P_l

Recoil polarization

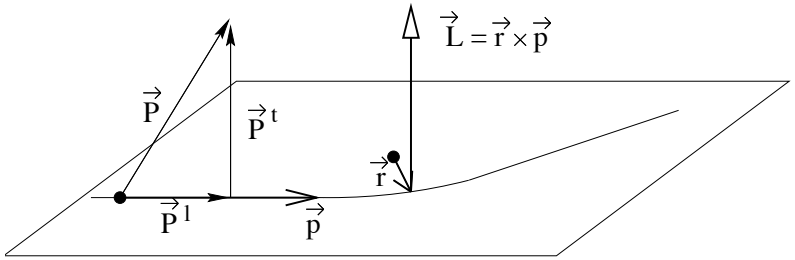

Elastic scattering of polarised nucleons on unpolarised protons has analysing power $\epsilon(\theta_n)$ due to spin-orbit term V_{LS} in NN interaction.

Left-right asymmetry is observed if the proton is polarized vertically.

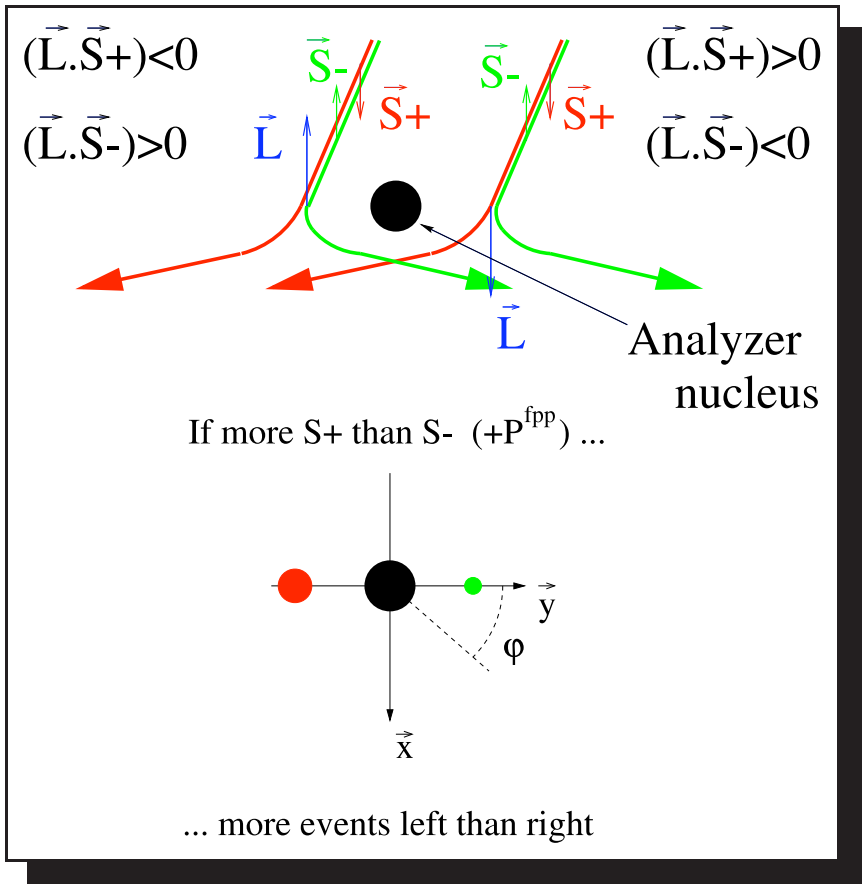

Recoil Polarization – Principle and Practice

- Interested in transfered polarization, P_l and P_t, at the target
- Polarimeters are sensitive to the perpendicular components only, P_n^{pol} and P_t^{pol}

  Measuring the ratio P_t/P_l requires the precession of P_l by angle χ before the polarimeter.
- If polarization precesses χ (e.g. in a dipole):
  $P_n^{\text{pol}} = \sin\chi \cdot hP_l$ and $P_t^{\text{pol}} = hP_t$

  $P_t^{\text{pol}} = P_t$ in scattering plane and proportional to $G_E G_M$

  P_n^{pol} is related to G_M^2
- G_E^p/G_M^p via $^1\text{H}(\vec{e}, e'\vec{p})$ at Jefferson Lab and Mainz
- G_E^n/G_M^n via $^2\text{H}(\vec{e}, e'\vec{n})p$ at Jefferson Lab and Mainz

G_E^p at Jefferson Lab (Hall A)

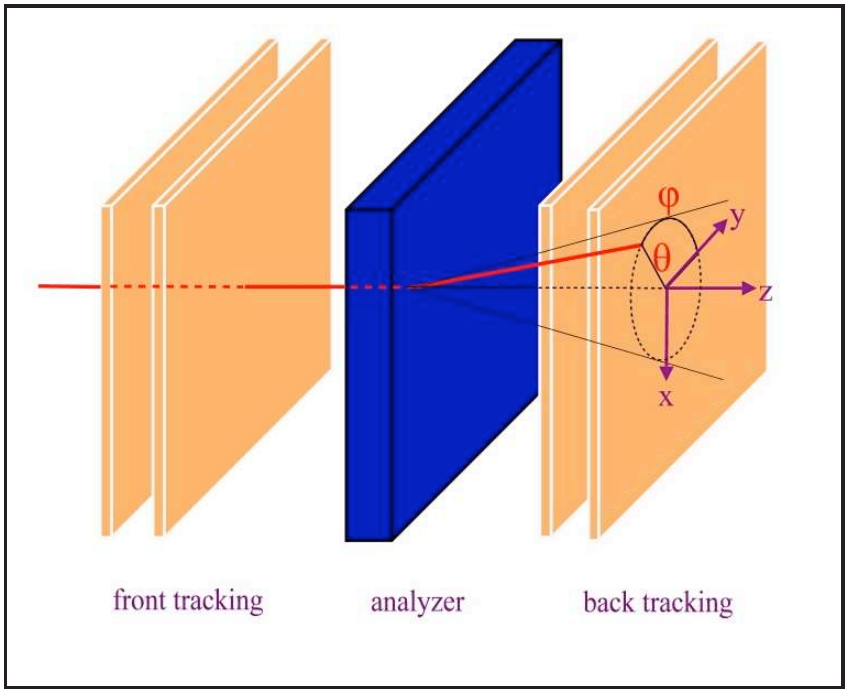

- left–right asymmetry $\Rightarrow P_n^{\text{fpp}}$ polarization in vertical direction
- up–down asymmetry $\Rightarrow P_t^{\text{fpp}}$ polarization in the horizontal direction

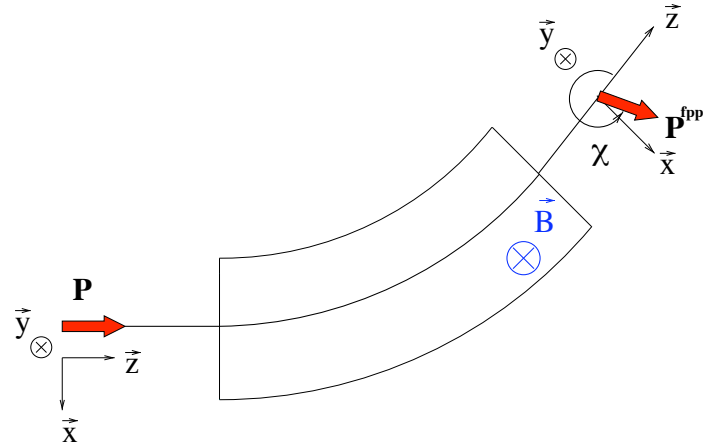

$$P_n^{\text{fpp}} = \sin\chi \cdot hP_l$$
$$P_t^{\text{fpp}} = hP_t$$
$$\chi = \gamma\theta_B(\mu_p - 1)$$

G_E^p in Hall A

Azimuthal Distribution

$$N(\vartheta,\varphi) = N_0(\vartheta)\epsilon(\vartheta)\left\{1 + \left[hA_y(\vartheta)P_t^{\text{fpp}} + a_{\text{instr}}\right]\sin\varphi - \left[hA_y(\vartheta)P_n^{\text{fpp}} + b_{\text{instr}}\right]\cos\varphi\right\}$$

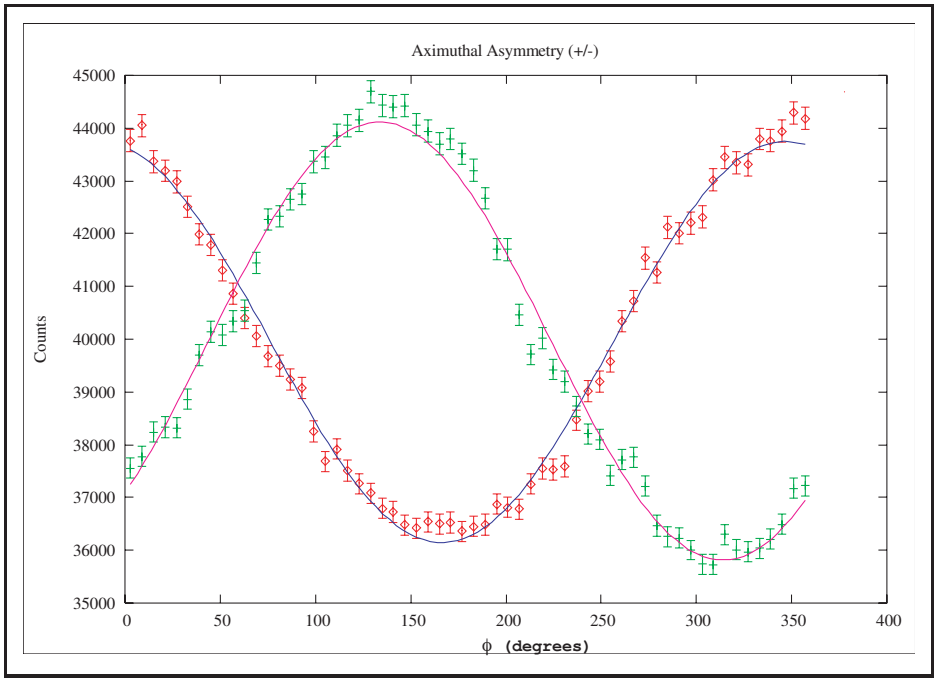

- Difference between 2 helicity states
  - instrumental asymmetries cancel, P_B and A_y cancel.
  - gain access to the polarization components $\frac{G_E}{G_M} = -\frac{P_t}{P_l}\frac{(E_e+E_{e'})}{2M_N}\tan(\frac{\theta_e}{2})$

G_E^p in Hall A – Results

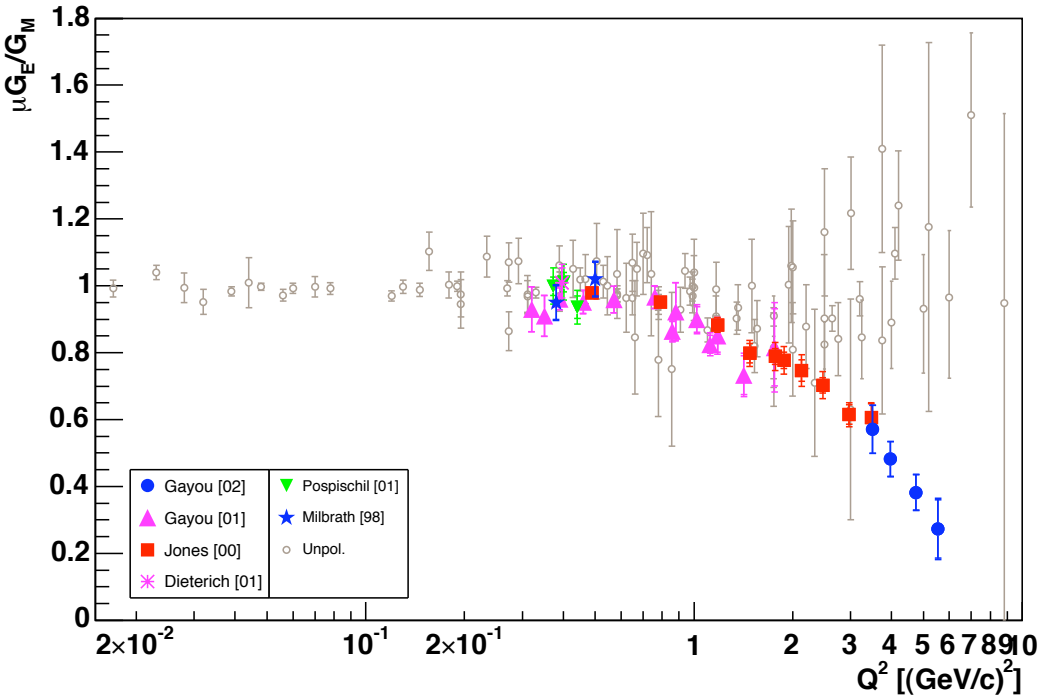

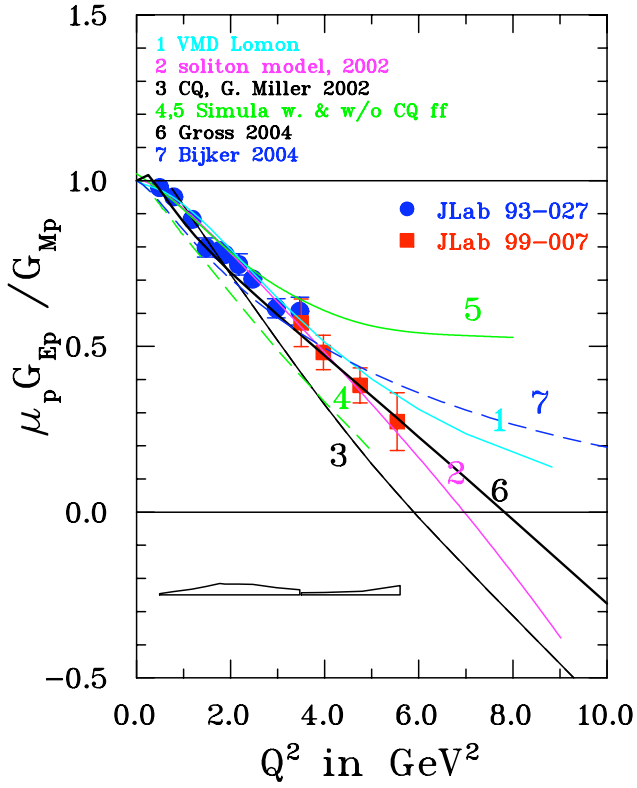

Ratio of G_E^p/G_M^p falls steeply with Q^2, in contrast with Rosenbluth measurements.

Problem with Rosenbluth technique or data? More later

G_E^p in Hall A – Results

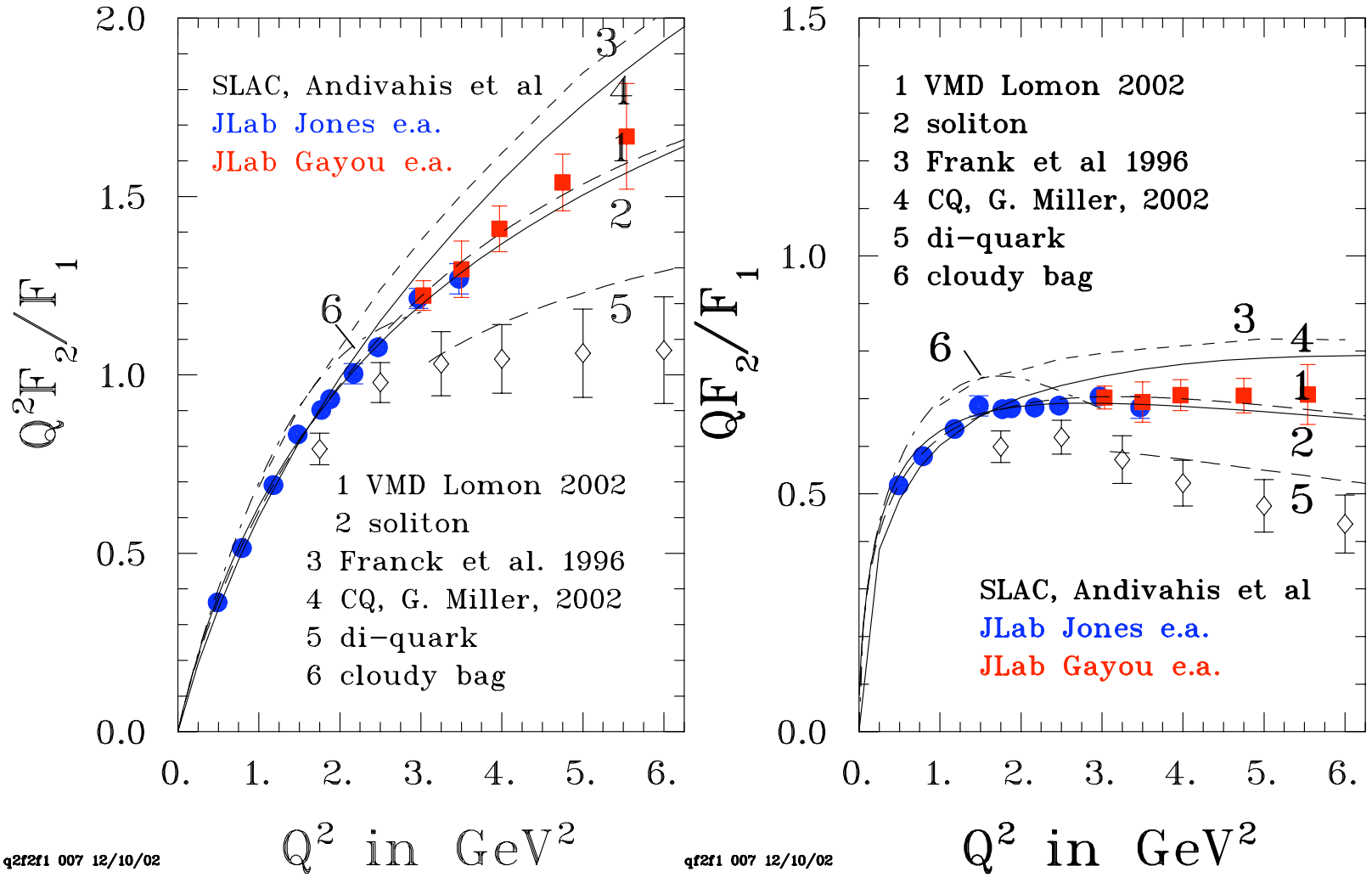

Interpretation

Considerable Attention - The two experiments have generated 100's of citations.

Popular press - New York Times, USA Today, Science News...

What is the Shape of the Proton? G. Miller, RCQM

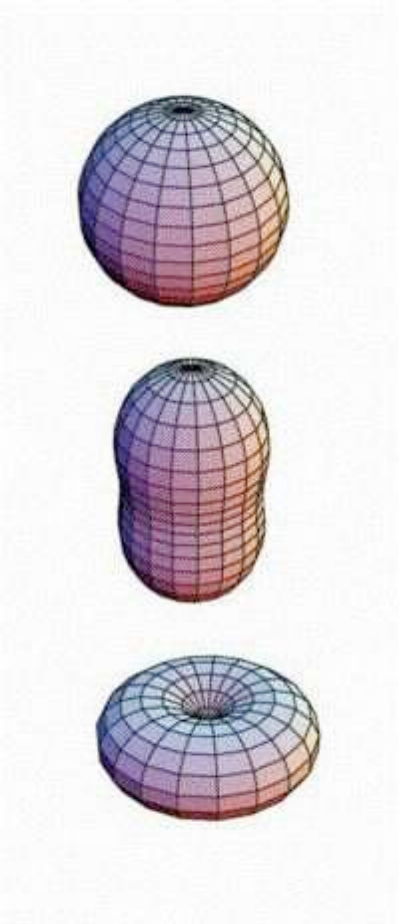

Momentum space representation, "normal" proton

High momentum quarks with spin aligned with proton

High momentum quarks with spin opposite to proton

G_E^n through recoil polarization

Recoil polarization, $^2\mathrm{H}(\vec{e}, e'\vec{n})p$, Mainz & JLAB

- In quasifree kinematics, $P_{s'}$ is sensitive to G_E^n and insensitive to nuclear physics
- Up–down asymmetry $\xi \Rightarrow$ transverse (sideways) polarization $P_{s'} = \xi_{s'}/P_e A_{\mathrm{pol}}$. Requires knowledge of P_e and A_{pol}
- Rotate the polarization vector in the scattering plane (with dipole magnet) and measure the longitudinal polarization, $P_{l'} = \xi_{l'}/P_e A_{\mathrm{pol}}$
- Take ratio, $\frac{P_{s'}}{P_{l'}}$. P_e and A_{pol} cancel
- E93038 at JLAB's Hall C: Three momentum transfers, $Q^2 = 0.45, 1.13,$ and $1.45(\mathrm{GeV/c})^2$.
- A1 Collaboration at Mainz: Three momentum transfers, $Q^2 = 0.3, 0.6$ and $0.8(\mathrm{GeV/c})^2$

Recoil polarization, $^2\mathrm{H}(\vec{e}, e'\vec{n})p$, Mainz & JLAB

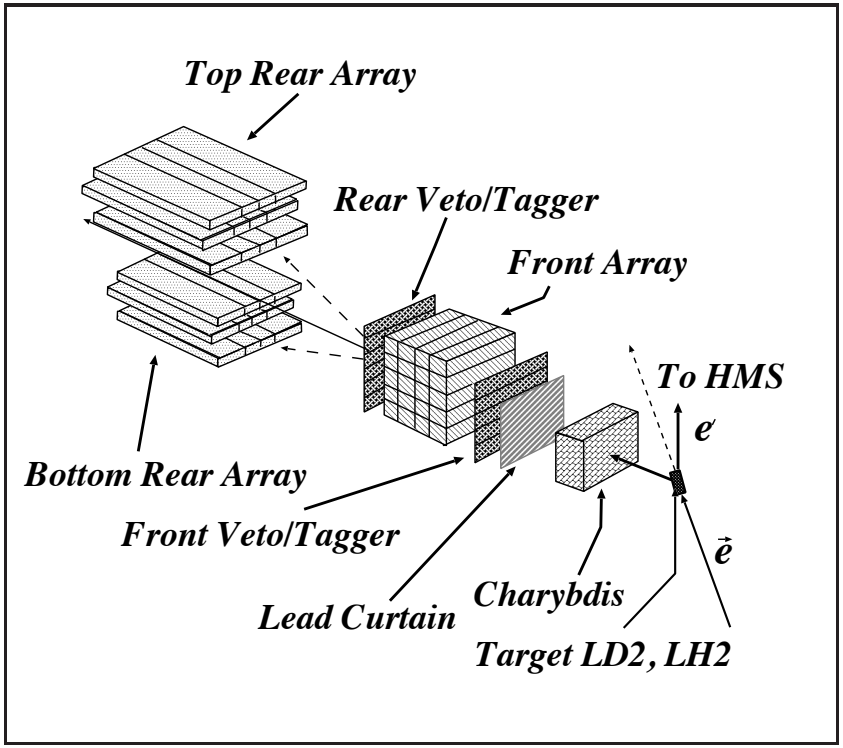

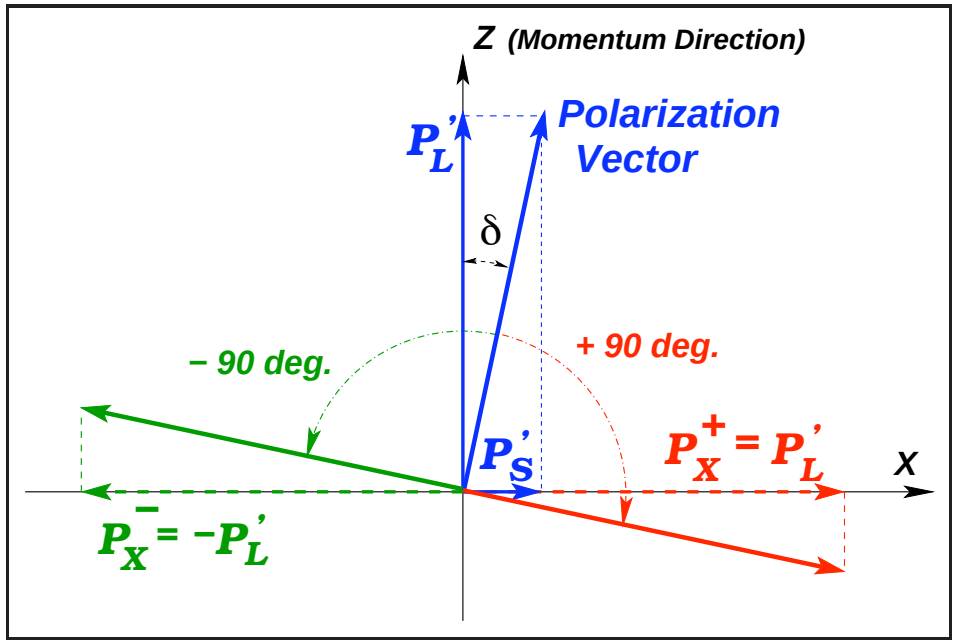

[Hall C]

Taking the ratio eliminates the dependence on the analyzing power and the beam polarization → greatly reduced systematics

$$\frac{G_E^n}{G_M^n} = K \tan\delta \qquad \text{where} \qquad \tan\delta = \frac{P_{s'}}{P_{l'}} = \frac{\xi_{s'}}{\xi_{l'}}$$

G_E^n via $^2\mathrm{H}(\vec{e}, e'\vec{n})p$

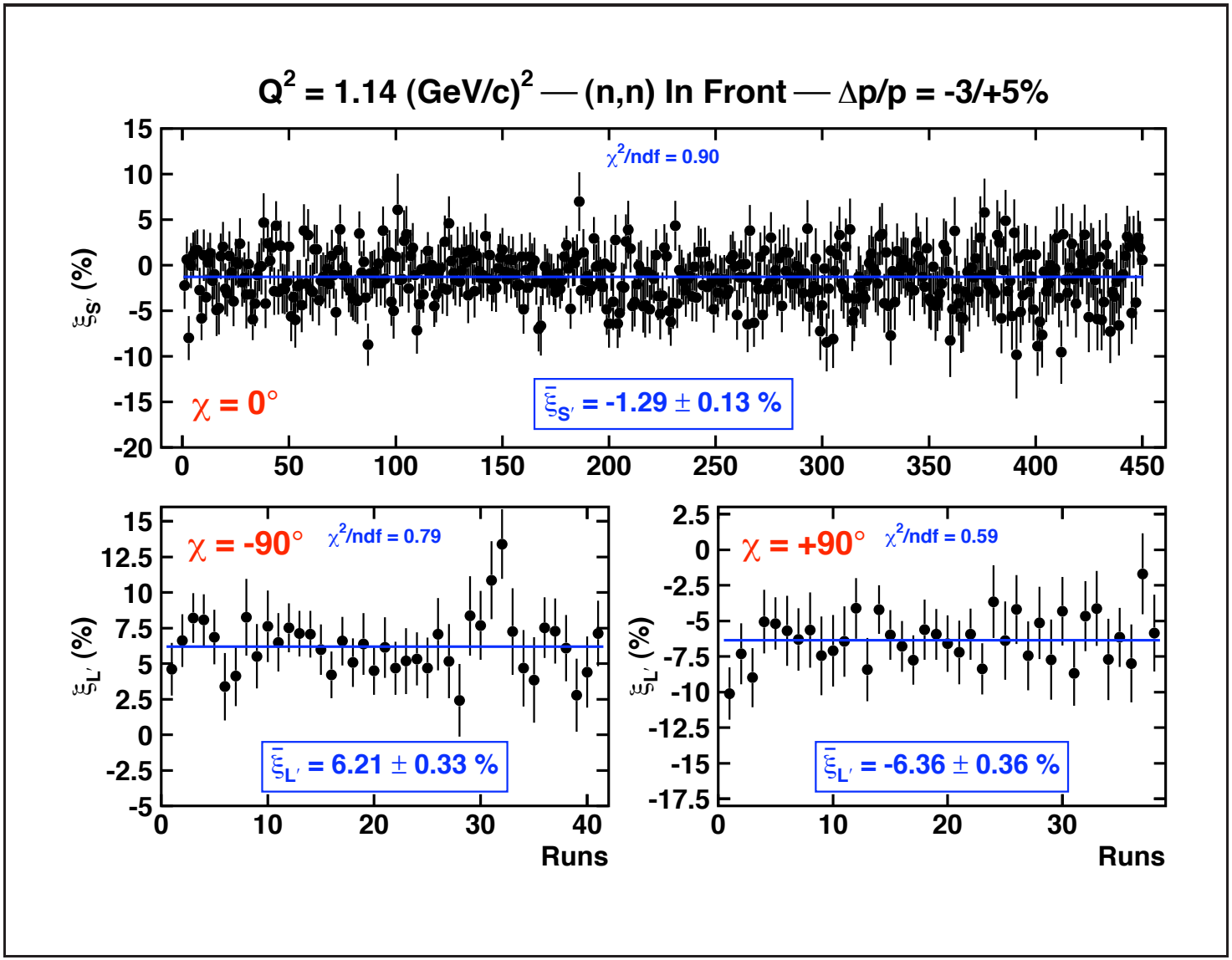

G_E^n via $^2\mathrm{H}(\vec{e}, e'\vec{n})p$

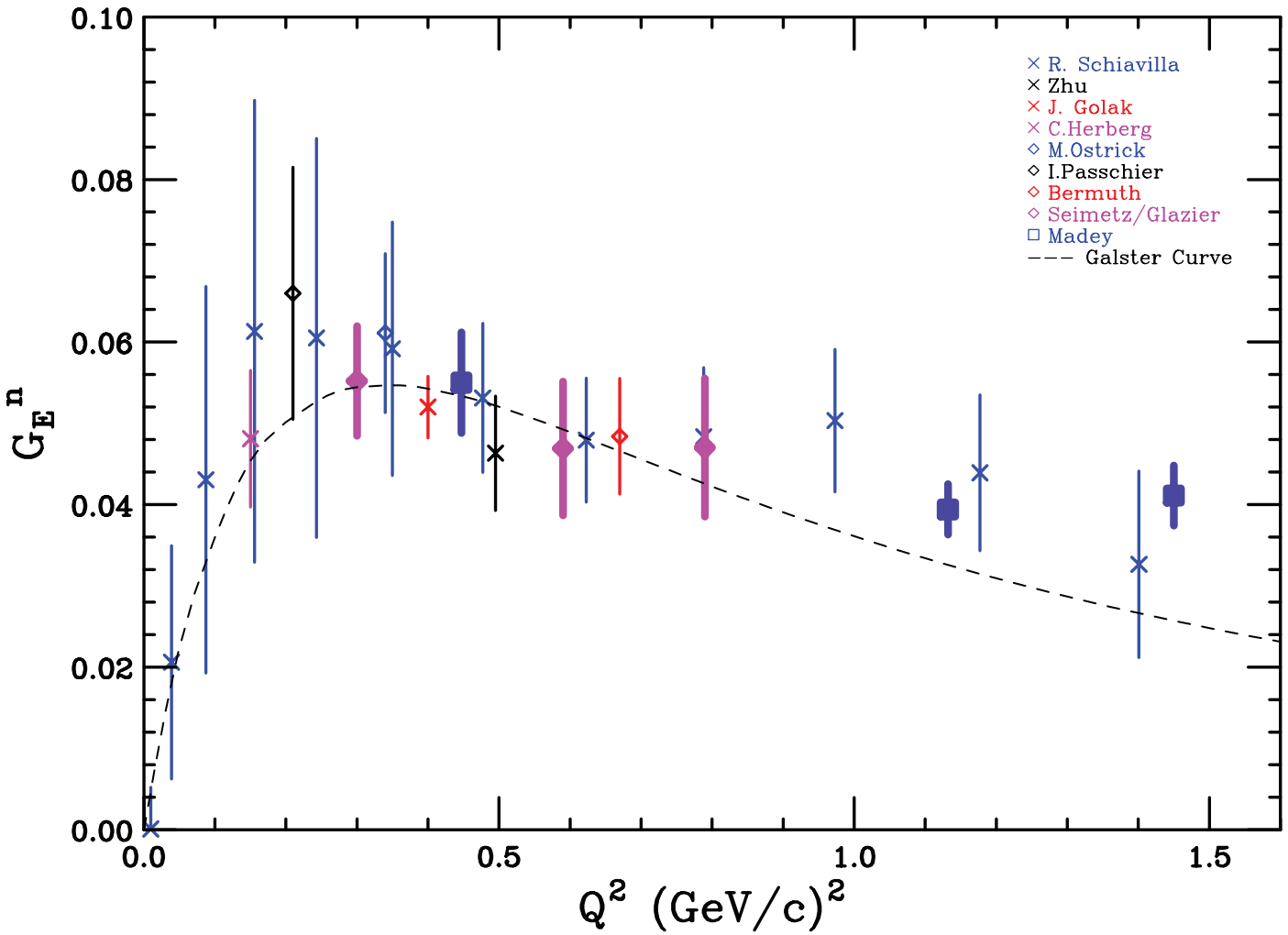

Beam–Target Asymmetry - Principle

Polarized Cross Section:

$\sigma = \Sigma + h\Delta$

Beam Helicity $h \pm 1$

$$A = \frac{\sigma_+ - \sigma_-}{\sigma_+ + \sigma_-} = \frac{\Delta}{\Sigma}$$

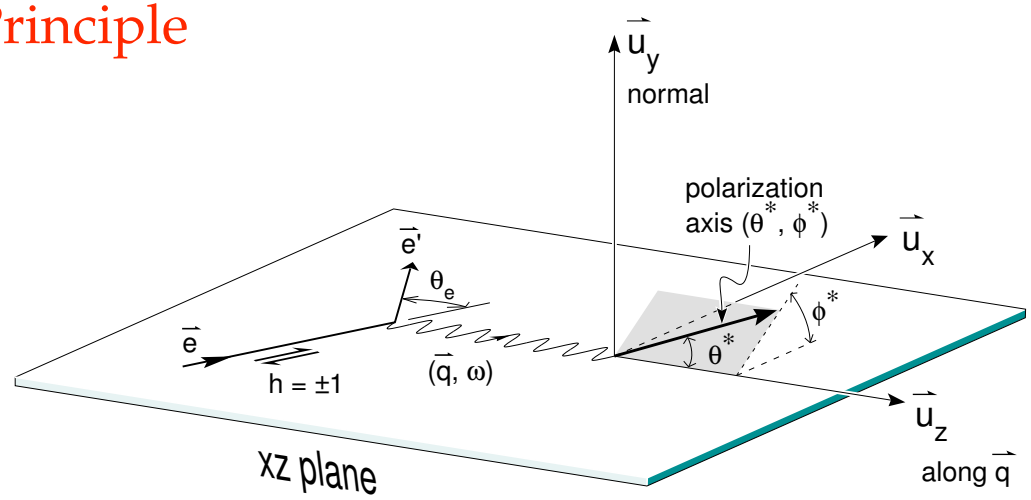

$$A = \frac{\overbrace{a\cos\Theta^\star (G_M)^2}^{A_T} + \overbrace{b\sin\Theta^\star\cos\Phi^\star G_E G_M}^{A_{TL}}}{c\,(G_M)^2 + d\,(G_E)^2}; \quad \varepsilon = \frac{N^\uparrow - N^\downarrow}{N^\uparrow + N^\downarrow} = P_B \cdot P_T \cdot f \cdot A$$

$\Theta^\star = 90^\circ \quad \Phi^\star = 0^\circ$

$$\Longrightarrow A_{TL} = \frac{bG_E G_M}{c\,(G_M)^2 + d\,(G_E)^2}$$

$\Theta^\star = 0^\circ \quad \Phi^\star = 0^\circ$

$$\Longrightarrow A_T = \frac{aG_M^2}{c\,(G_M)^2 + d\,(G_E)^2}$$

JLAB, BLAST, Mainz $\overrightarrow{H}$, $\overrightarrow{^2\mathrm{H}}$, $\overrightarrow{^3\mathrm{He}}$

Beam–Target Asymmetry - Neutron

- No free neutron
- Unpolarized materials
- Protons dominate
- The deuteron and ^{3}He only approximate a polarized neutron
- Scattering from other polarized materials
- Indirect measurement of form factors
- Taking ratio of A_{TL}/A_T not always practical; errors arising from P_t and P_b

$\overrightarrow{\mathrm{D}}(\overrightarrow{e}, e'n)p$ $\quad \sigma(h,P) = \sigma_0\left(1 + hPA_{ed}^V\right)$

A_{ed}^V is sensitive to G_E^n

has low sensitivity to potential models

has low sensitivity to subnuclear degrees of freedom (MEC, IC)

in quasielastic kinematics

Sensitivity to G_E^n – Insensitivity to Reaction

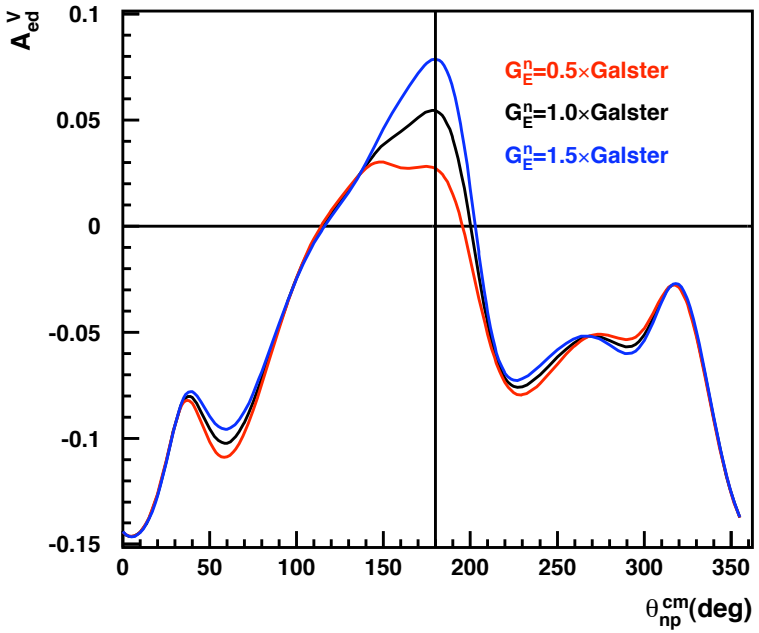

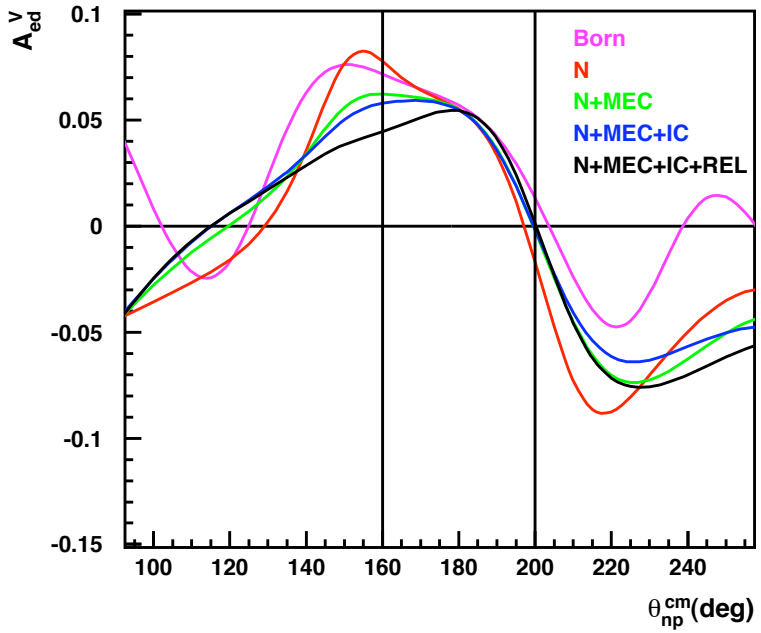

G_E^n in Hall C/BLAST via $\overrightarrow{^2\mathrm{H}}(\vec{e}, e'n)p$

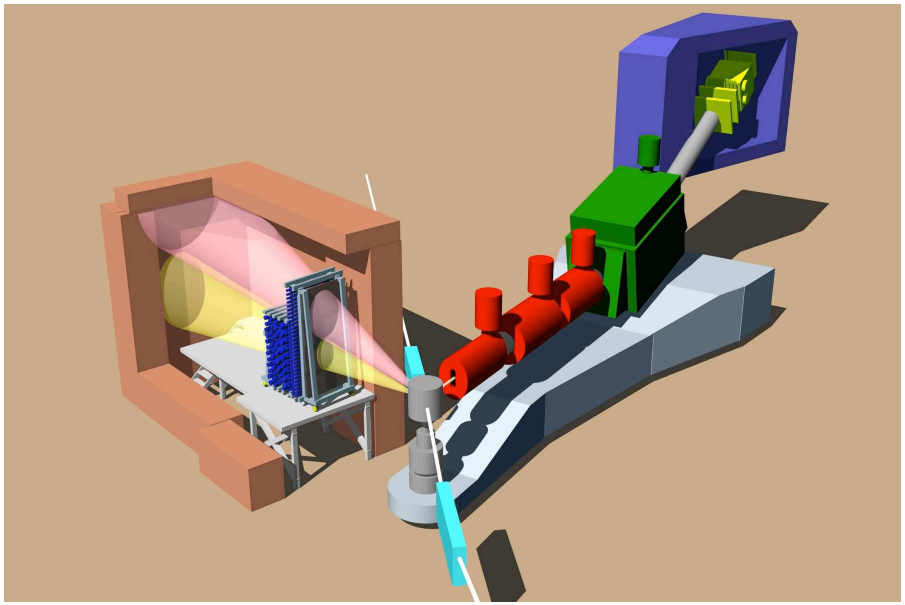

Solid Polarized Target
Electrons in HMS
Neutron detection
Charged PID: Veto Counters
Magnetic chicane

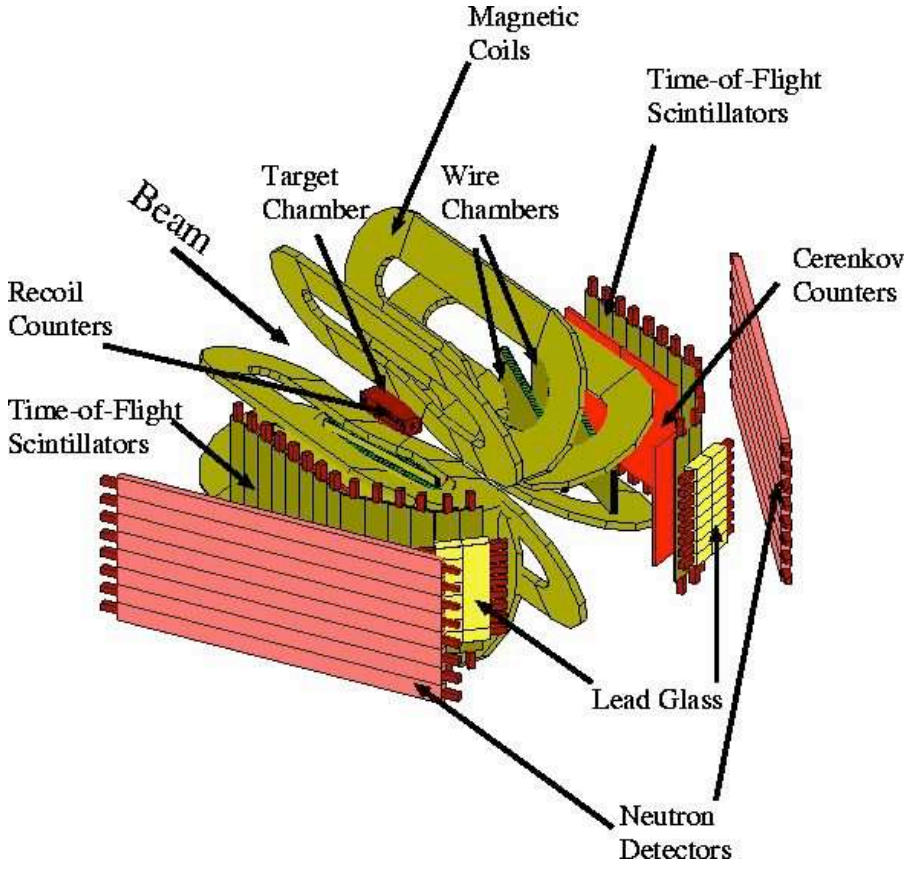

Internal Target
Polarized Atomic Beam Source
Very large acceptance
Neutron detection
Charged particle veto: DC

Neutron Detector

- Highly segmented scintillator
- Rates: 50 - 200 kHz per detector
- Pb shielding in front to reduce background
- 2 thin planes for particle ID (VETO)
- 6 thick conversion planes
- 142 elements total, >280 channels
- Extended front section for symmetric proton coverage
- PMTs on both ends of scintillator
- Spatial resolution $\simeq$ 10 cm
- Time resolution $\simeq$ 400 ps
- Provides 3 space coordinates, time and energy

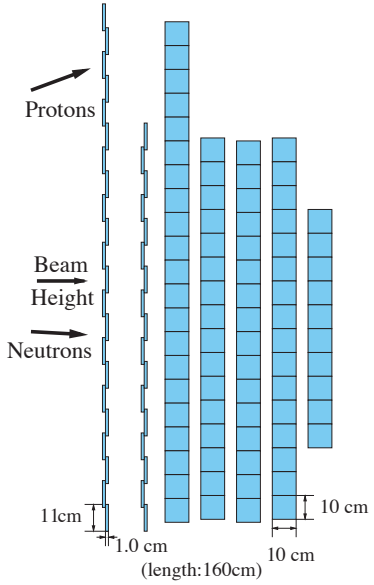

1998

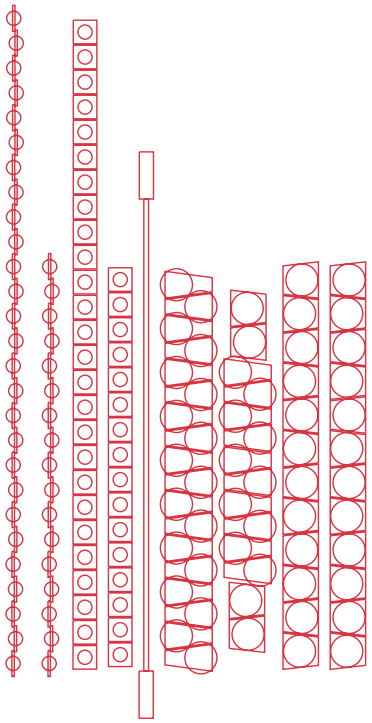

2001

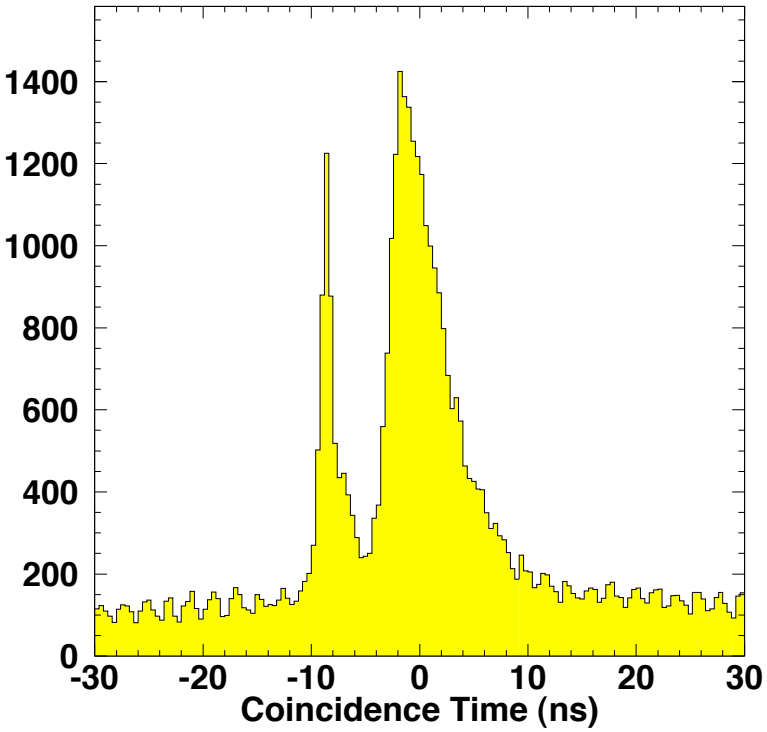

n Detector — Single Event Display

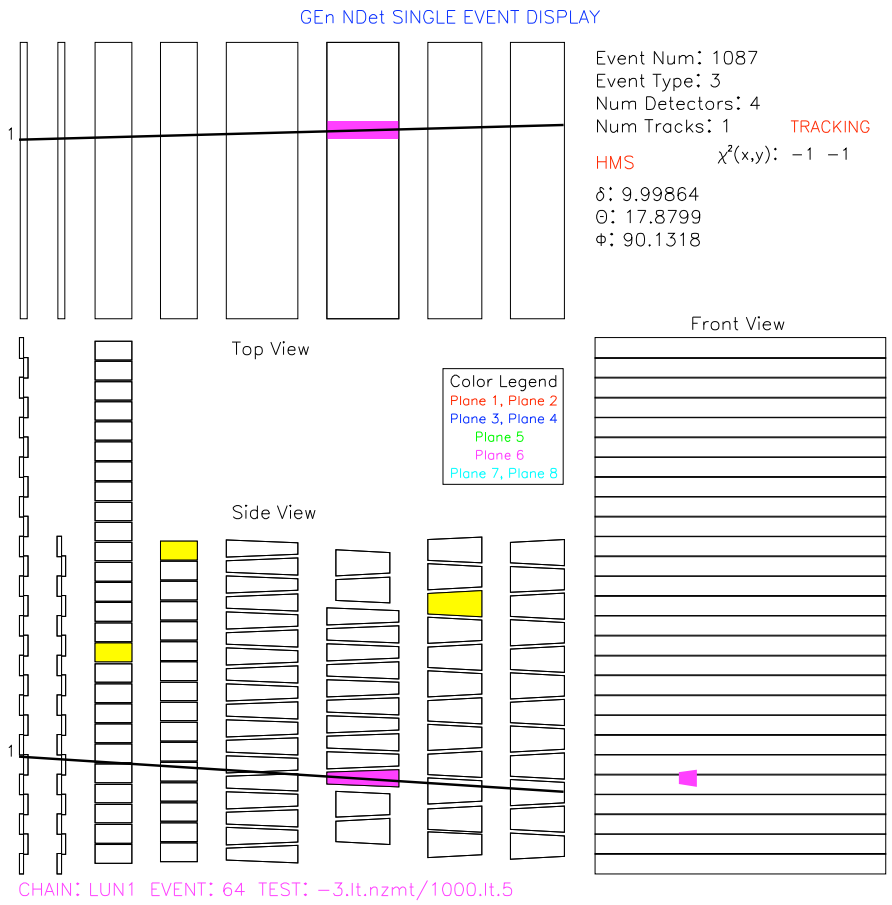

Sample Neutron Track

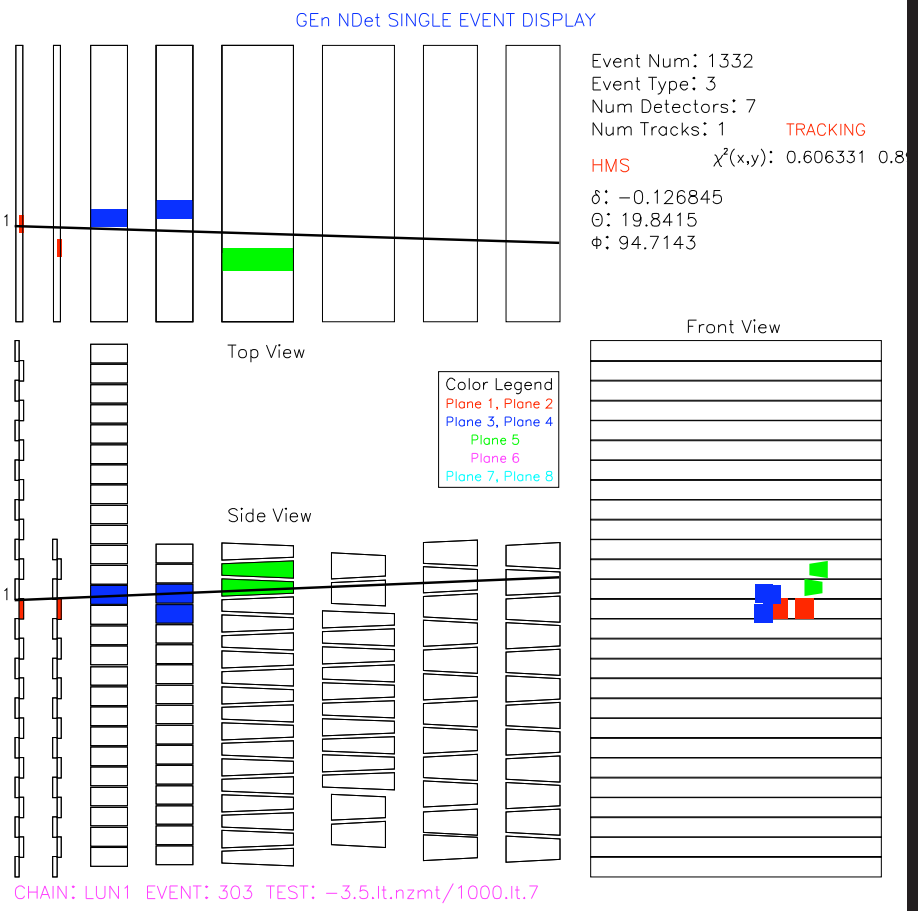

Sample Proton Track

majority of protons in upper half of detector

Data and Calculations of G_E^n

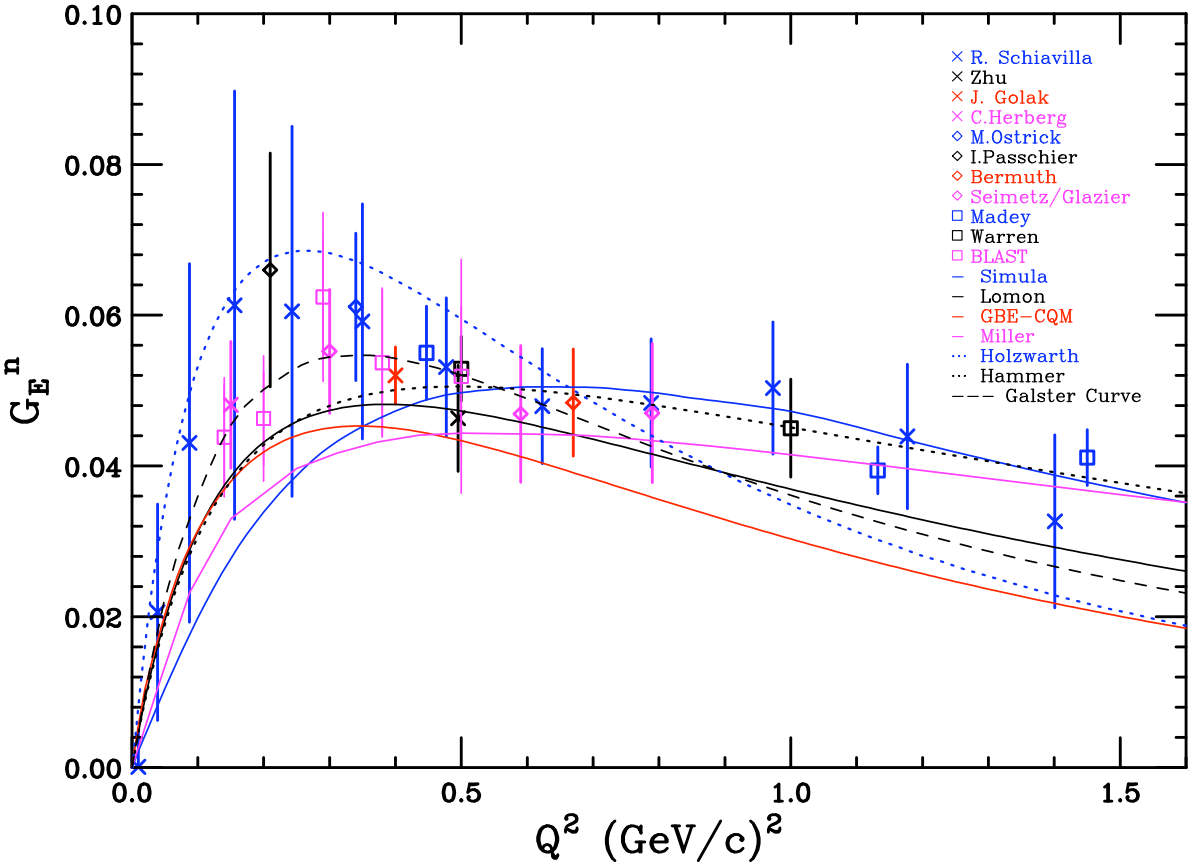

BLAST G_E^p/G_M^p Data via $\vec{\mathrm{H}}(\vec{e}, e'\, p)$

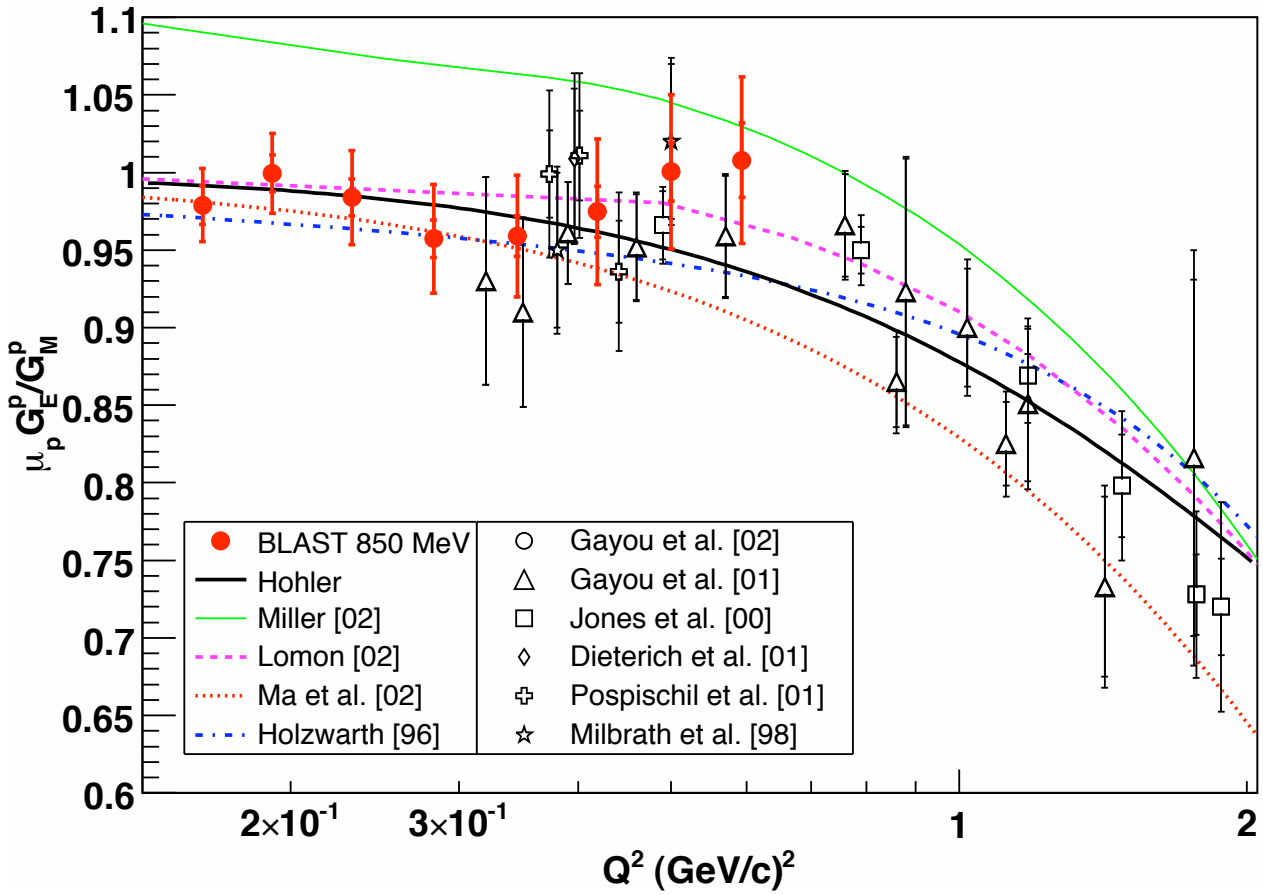

C. Crawford, thesis. Systematics are dominated by the reconstruction (knowledge of Q^2). Expectation is that the systematics will be reduced significantly in final analysis.

Latest G_M^n at low Q^2 from via $\overrightarrow{^2\mathrm{H}}(e,e')X$

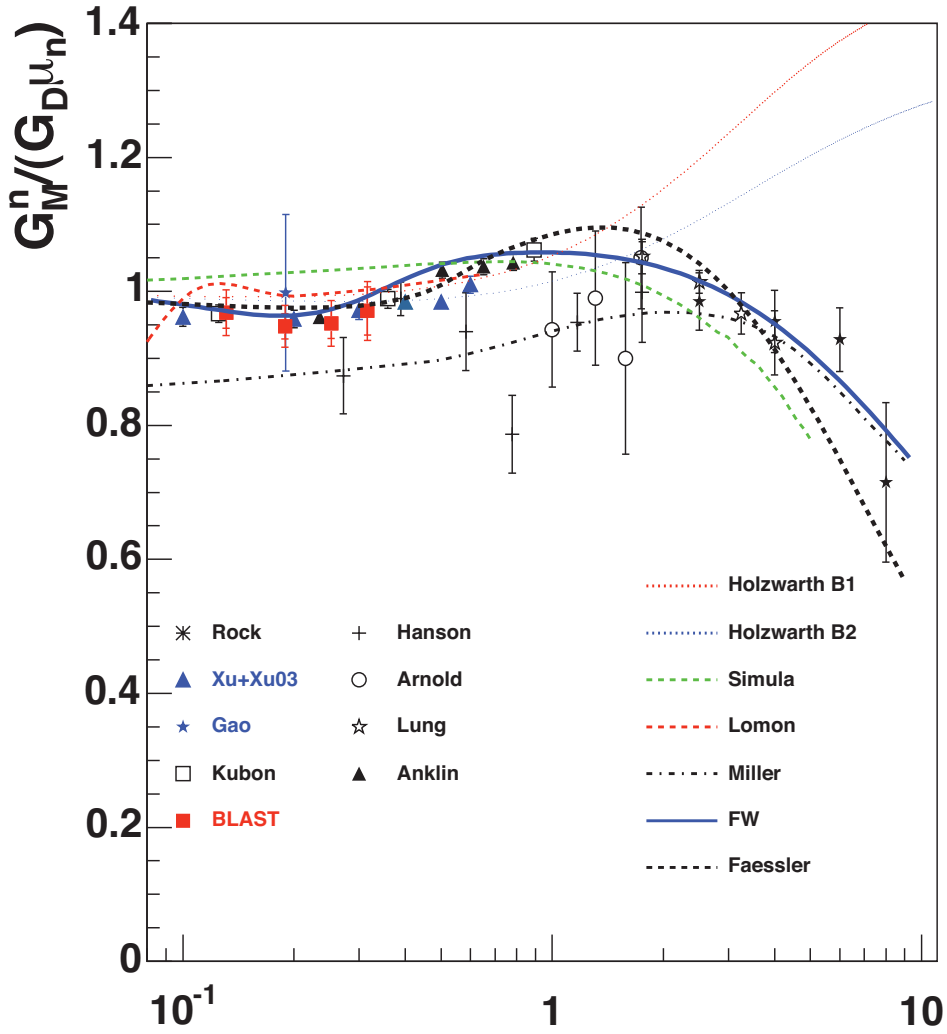

Latest (preliminary) data from BLAST using Atomic Beam Source

Excellent agreement with $\overrightarrow{^3\mathrm{He}}(e,e')X$ and ratio method data

Complete analysis of BLAST data set forthcoming.

G_M^n at High Q^2 in CLAS

$$R_D = \frac{\frac{d\sigma}{d\Omega}^{D(e,e'n)p}_{QE}}{\frac{d\sigma}{d\Omega}^{D(e,e'p)n}_{QE}} \approx \frac{f(G_M^n, G_E^n)}{f(G_M^p, G_E^p)}$$

Has advantages over $D(e,e')$, $D(e,e'n)p$

- ✳ No Rosenbluth separation or subtraction of dominant proton
- ✳ Ratio insenstive to deuteron model
- ✳ MEC and FSI are small in quasielastic region

✓ Large acceptance to veto events with extra charged particles

✓ Data taken with hydrogen and deuterium target simultaneously

✓ Precise determination of neutron detection efficiency by via $H(e,e'n\pi^+)$

G_M^n Preliminary results from CLAS

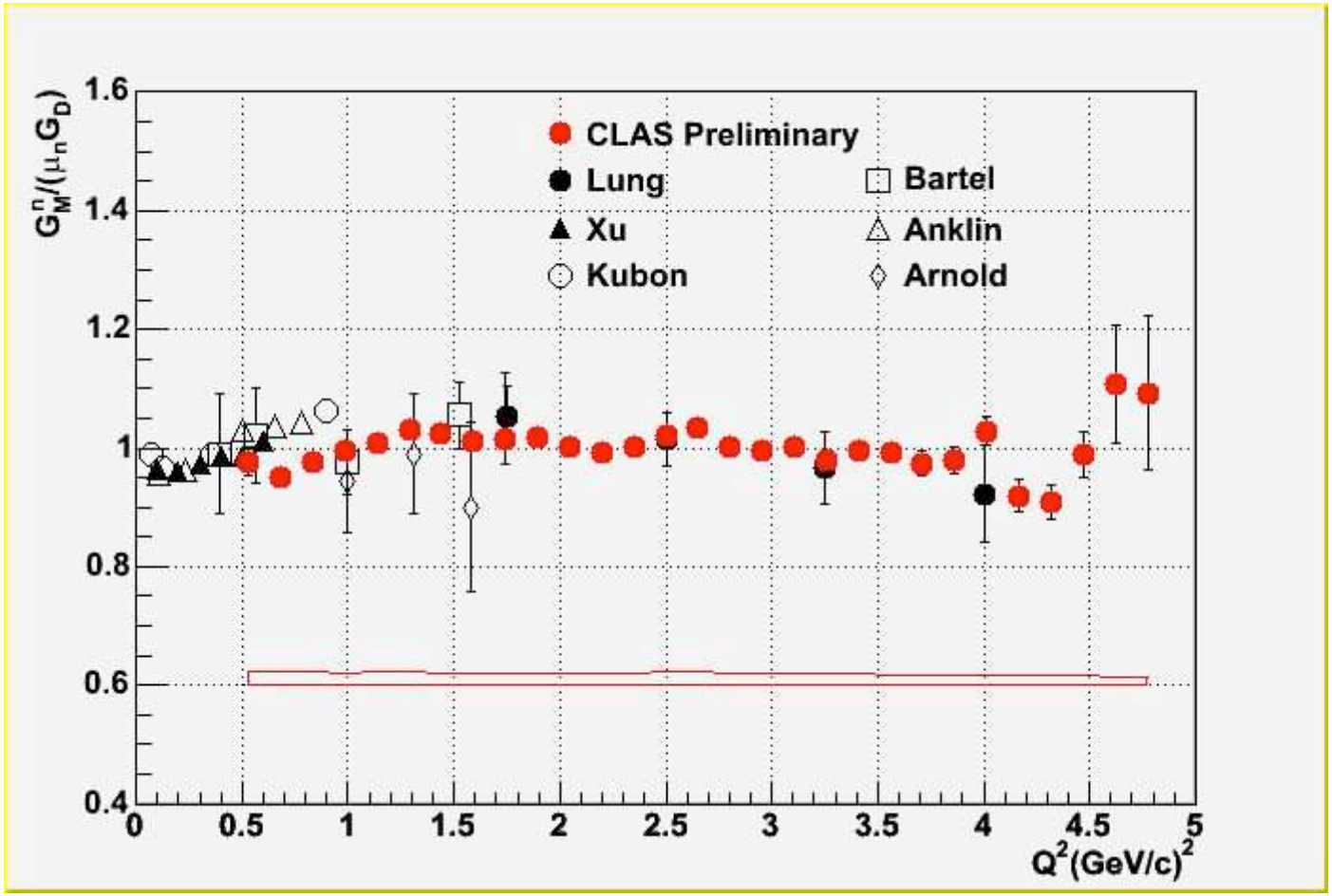

Preliminary results show a minimal deviation from dipole

Pion Cloud

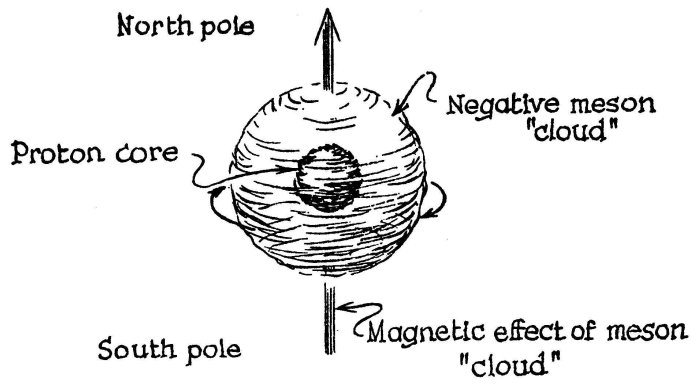

Friedrich & Walcher remphasized role of pion cloud. They fit all form factors consistently as a sum of a broad distribution and a "bump", where the "bump" is due to a π-cloud. The "bump" shows up in all 4 form factors at $Q^2 \simeq 0.25$ [Kaskulov & Grabmayr, Miller]

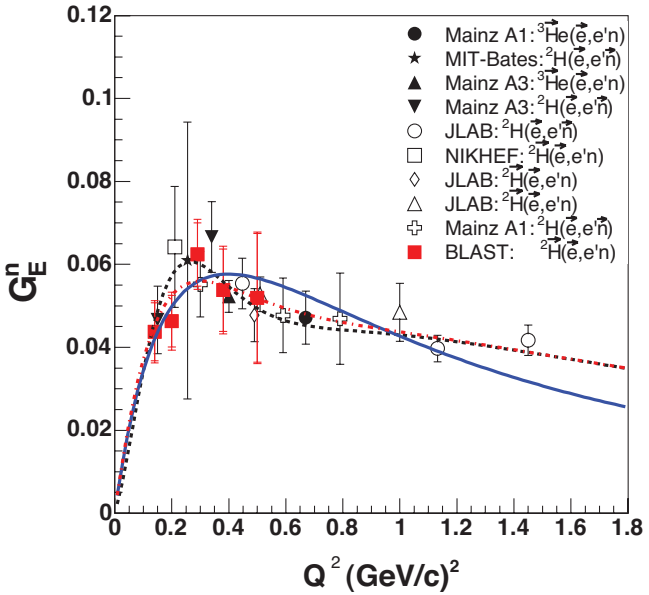

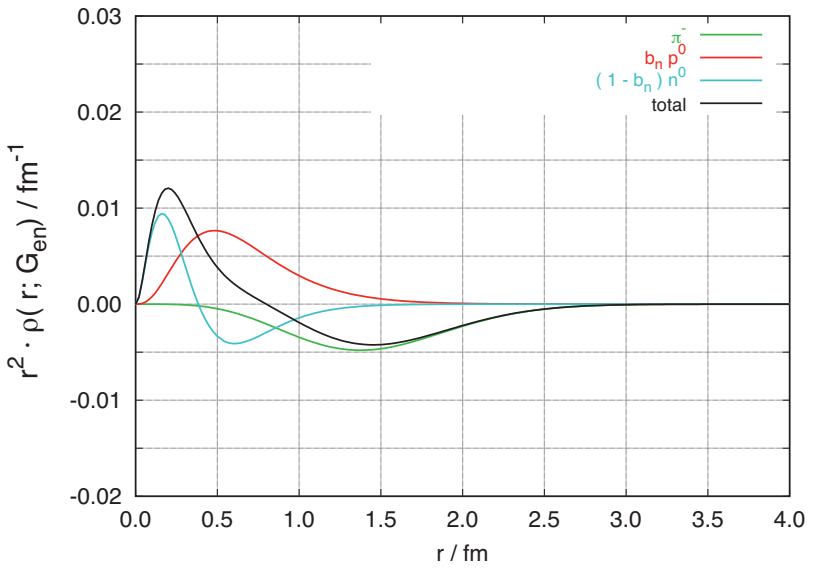

G_E^p , Status of Rosenbluth Separations

$$\sigma_R \equiv \frac{d\sigma}{d\Omega}\frac{\epsilon(1+\tau)}{\sigma_{Mott}} = \tau G_m^2(Q^2) + \epsilon G_E^2(Q^2)$$

Fundamental problem: σ insensitive to G_E^p at large Q^2. With $\mu G_E^p = G_M^p$, G_E^p contributes 8.3% to total cross section at $Q^2 = 5$.

$$\delta G_E \propto \delta(\sigma_R(\epsilon_1) - \sigma_R(\epsilon_2))(\Delta\epsilon)^{-1}(\tau G_M^2/G_E^2)$$

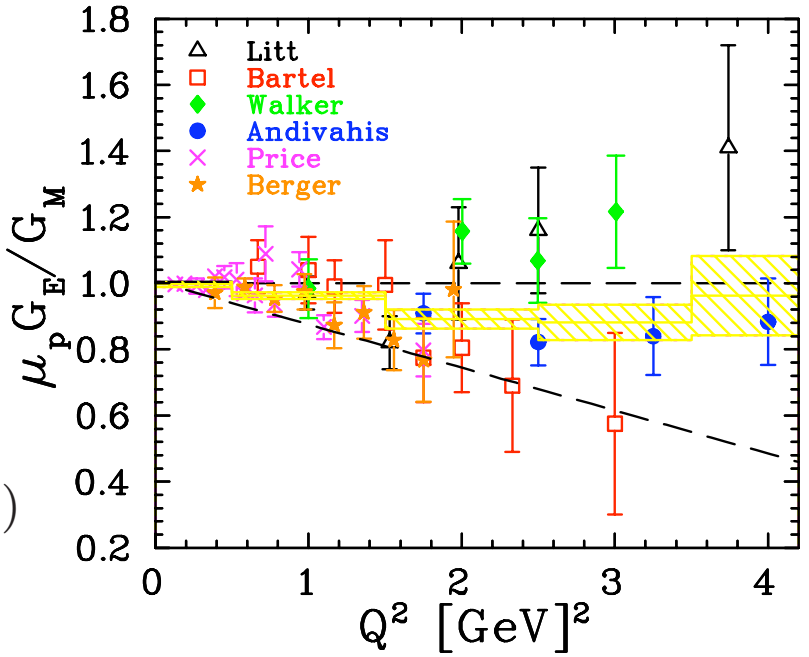

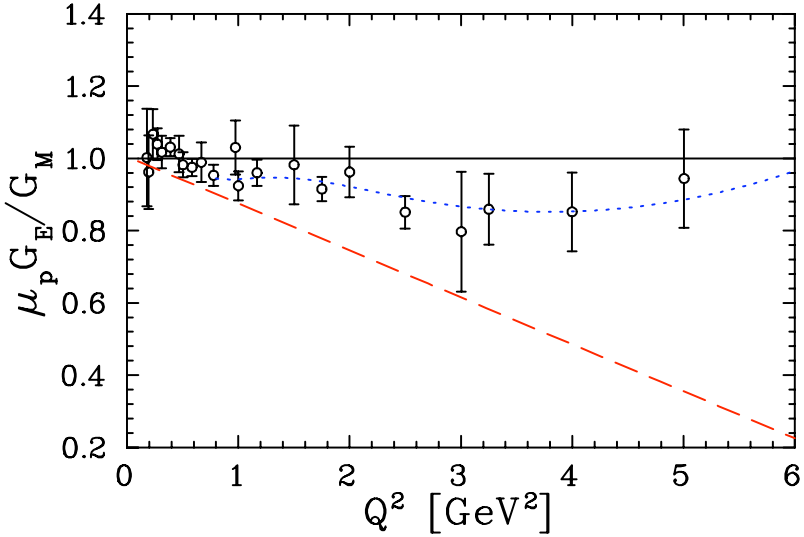

J. Arrington:

Phys. Rev. C68:034325, 2003

- E94-110 consistent with global fit
- Rules out experimental systematics
- ϵ dependence must be large
- Unconsidered ϵ dependent radiative correction

Super–Rosenbluth, $p(e,p)$

Reduces size of dominant corrections

Rate nearly constant for protons

No p dependent systematics

Sensitivity to angle momentum reduced

Luminosity monitor (second arm)

Background small

Qattan *et al.* Phys. Rev. Lett. 94:142301, 2005 (nucl-ex/0410010)

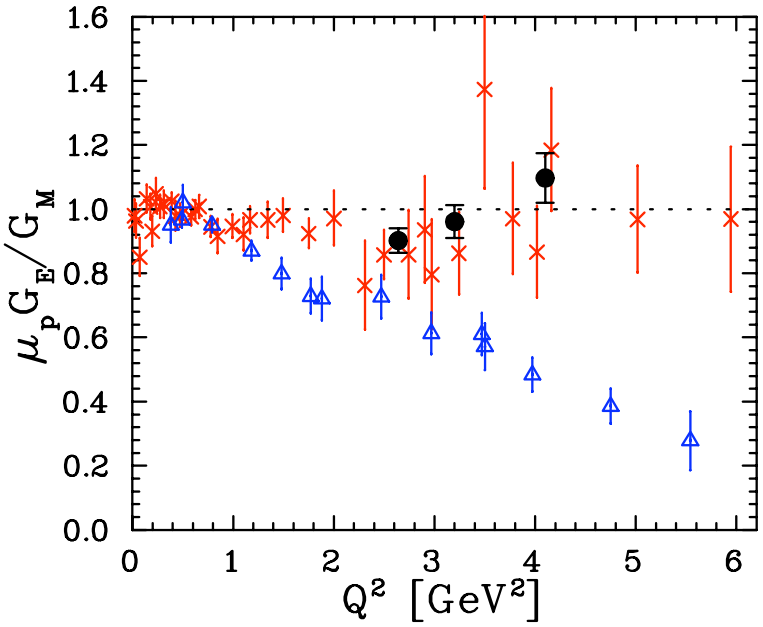

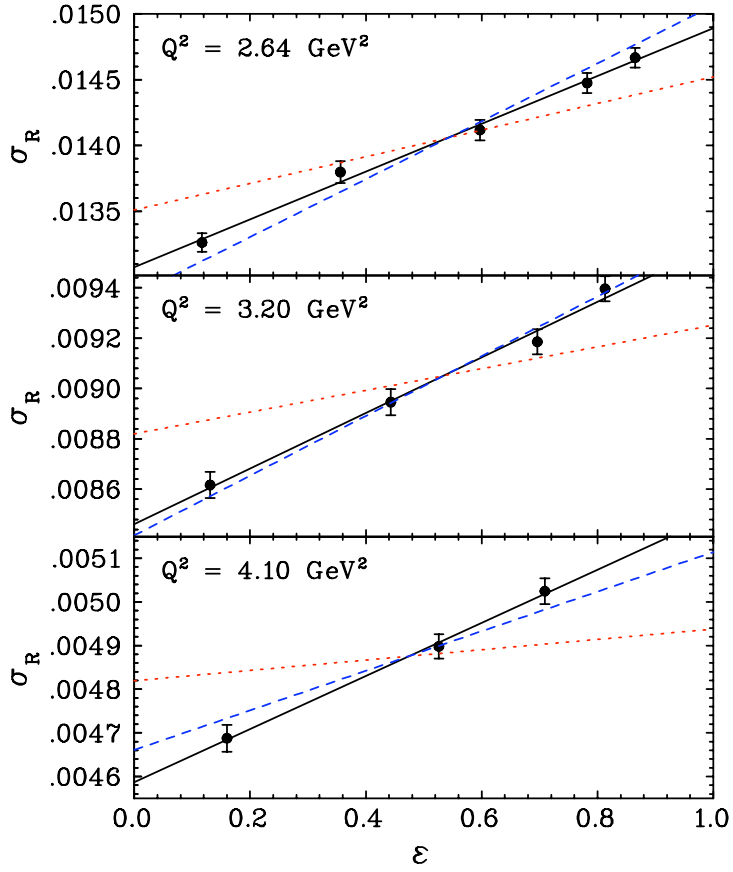

Possible explanation: radiative corrections

There are radiative corrections to Rosenbluth experiments that are not included in the analysis

These corrections are: Linear in ϵ and only weakly Q^2 dependent.

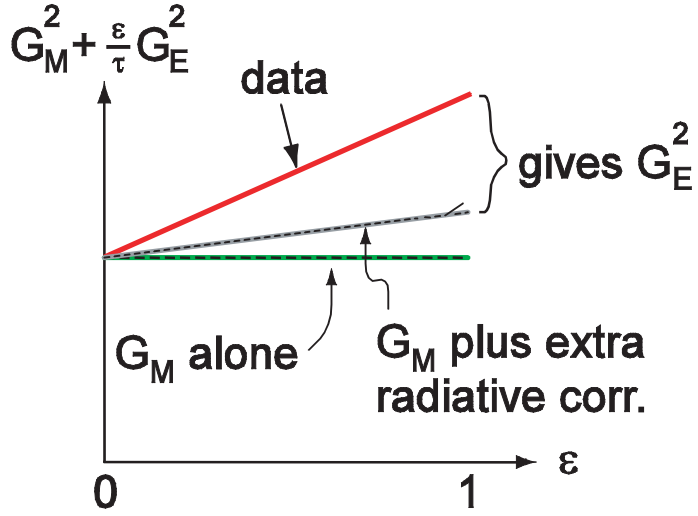

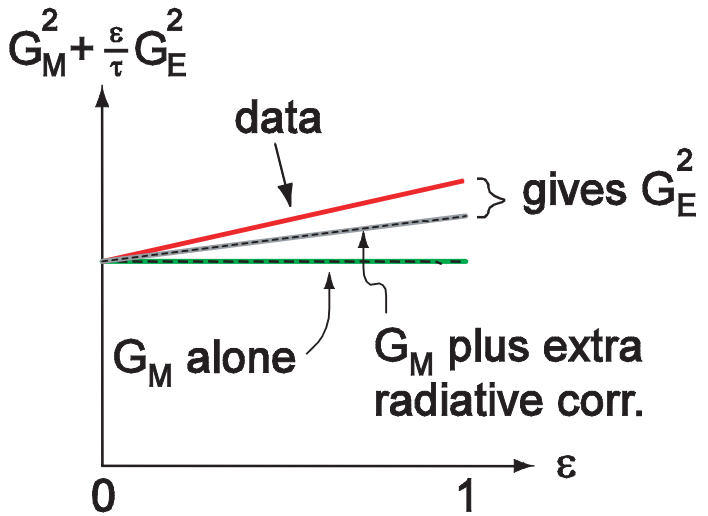

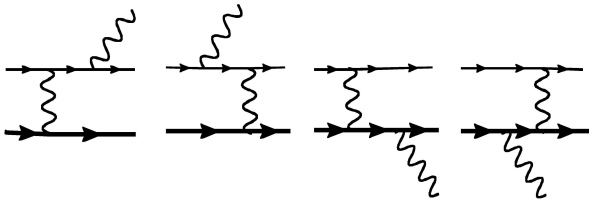

bremsstrahlung

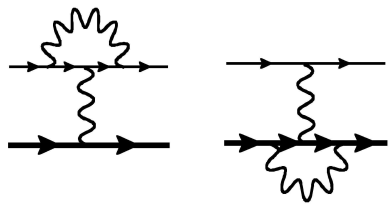

vertex corrections

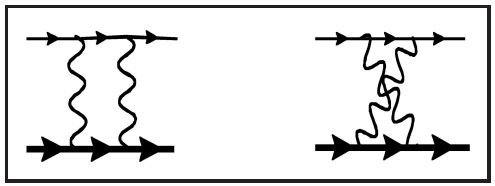

Two-photon exchange

Two Photon Contributions

Chen, Afanasev, *et al.* approach:

- → hard scattering from quark
- → GPDs describe the quark emission and absorption
- ✔ They argue that when taking the PT form factors as input the addition of the 2–photon correction reproduces the Rosenbluth data
- → PRL 93, 122301(2004), PRD 72 013008 (2005)

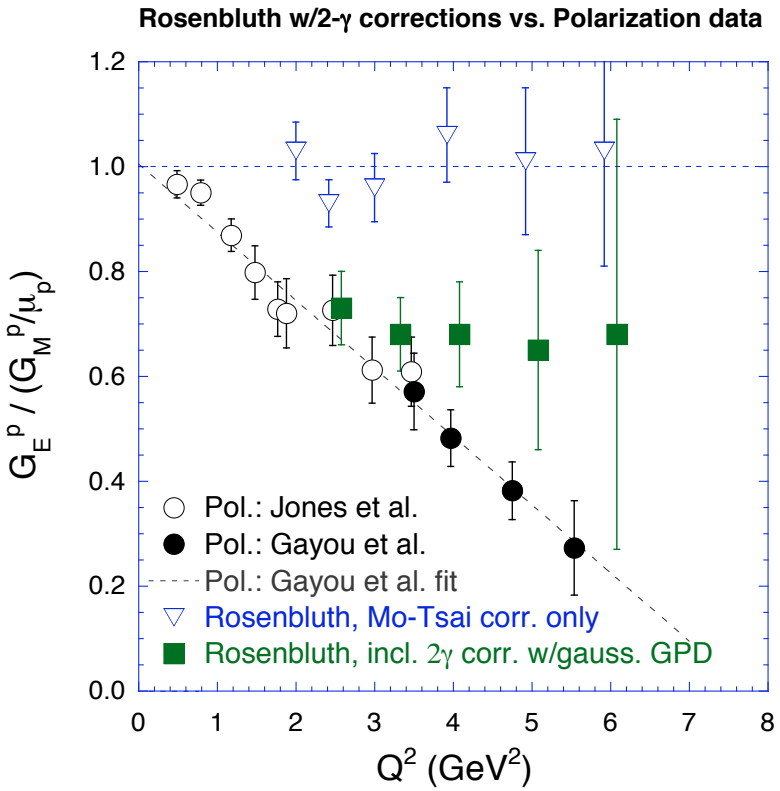

Other work by Tomasi and Rekalo and Blunden, Melnitchuk and Tjon

Two-Photon Contributions

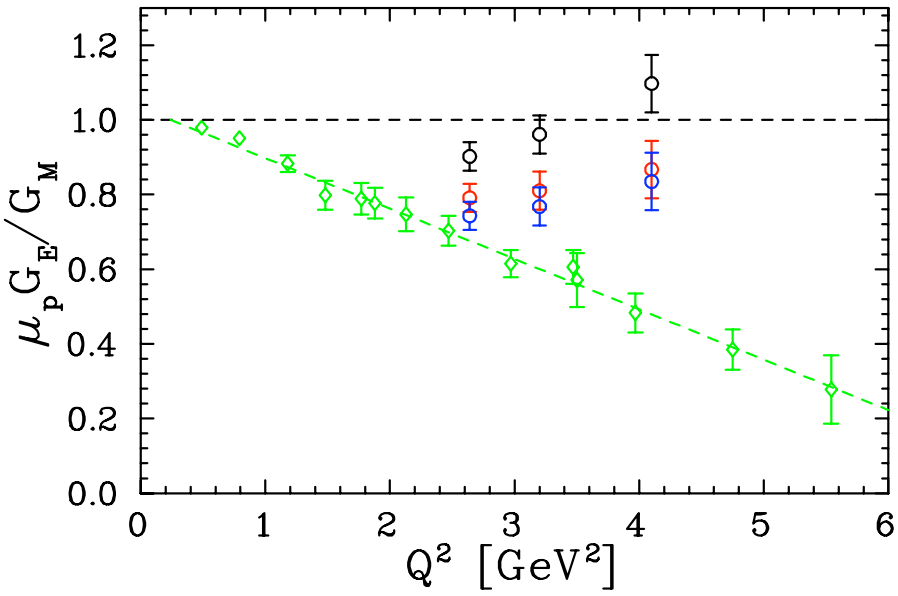

① E01-001 analysis

② TPE of Chen et al.

③ TPE and Coulomb correct. (nucl-ex/0406014)

④ Still a discrepancy, of which only one-half is explained

⑤ To date, no evidence of non-linearity in Rosenbluth data, V. Tvaskis et al,Phys.Rev.C73:025206,2006

Experimental Tests are Possible

- $\frac{\sigma(e^+p)}{\sigma(e^-p)}$ E-04-116
- Rosenbluth linearity E-05-017
- Recoil polarization, p_n
- ϵ dependence of polarization transfer E-04-019
- $\vec{p}^{\uparrow}(e,e')p$ (SSA)
- $\vec{p}(\vec{e},e')$

Two-Photon in other reactions

- Neutron from factors, G_E^n
- Weak form-factors
- Deuteron form factors

  See J. Arrington, Nucleon-05 contribution.

Notes on two-photon

e^+/e^- and A_y are due to interference of the real parts of the one and two photon terms. Recoil polarization is a measure of the imaginary part

Possible to use elastic electron-nucleon scattering to observe the T-odd parity conserving target single spin asymmetry. It is time reversal odd but A_y does not violate time-reversal invariance.

$A_y = \frac{\sigma_\uparrow - \sigma_\downarrow}{\sigma_\uparrow + \sigma_\downarrow}$

Single spin asymmetry A_y arises from interference between one-photon and two-photon exchange amplitudes and is sensitive to the two-photon exhange amplitude. The normal spin asymmetry is related to the absorptive part of the elastic eN scattering amplitude. Since the one-photon exchange amplitude is purely real, the leading contribution to A_y is of order $O(e^2)$, and is due to an interference between one- and two photon exchange amplitudes.

Data and Theory-VMD

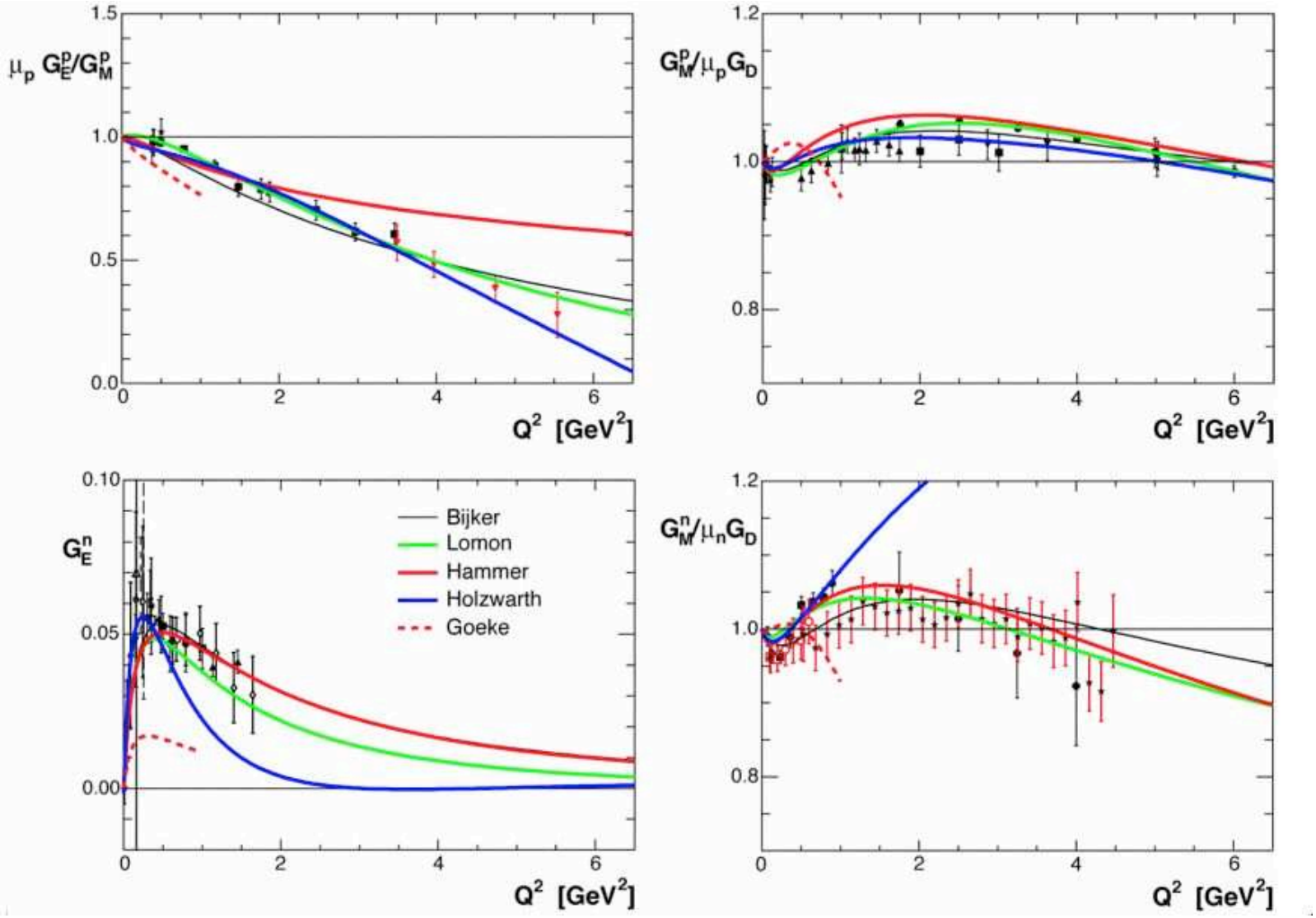

Data and Theory-RCQM

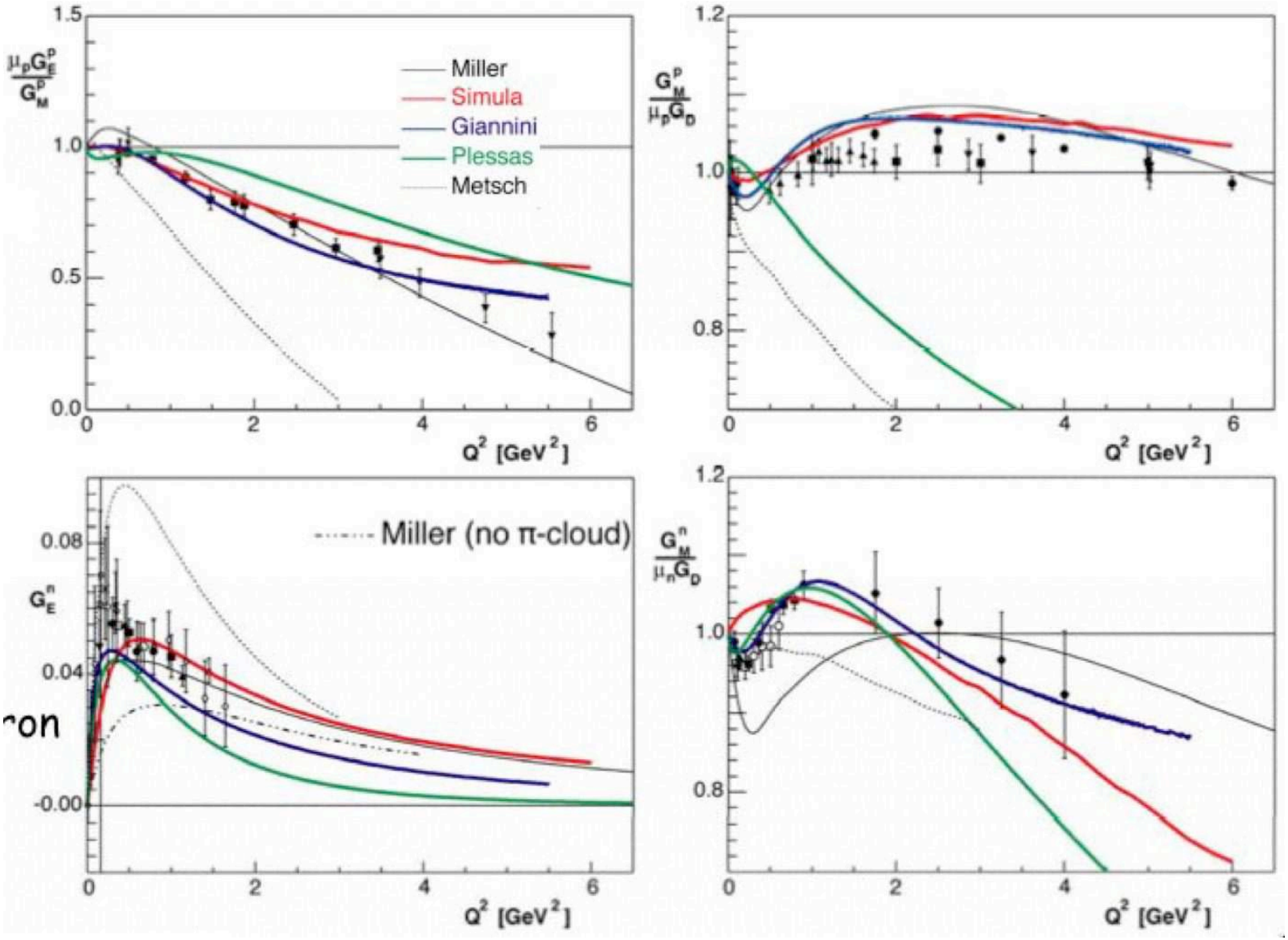

Data and Theory-Chiral Extrapolation

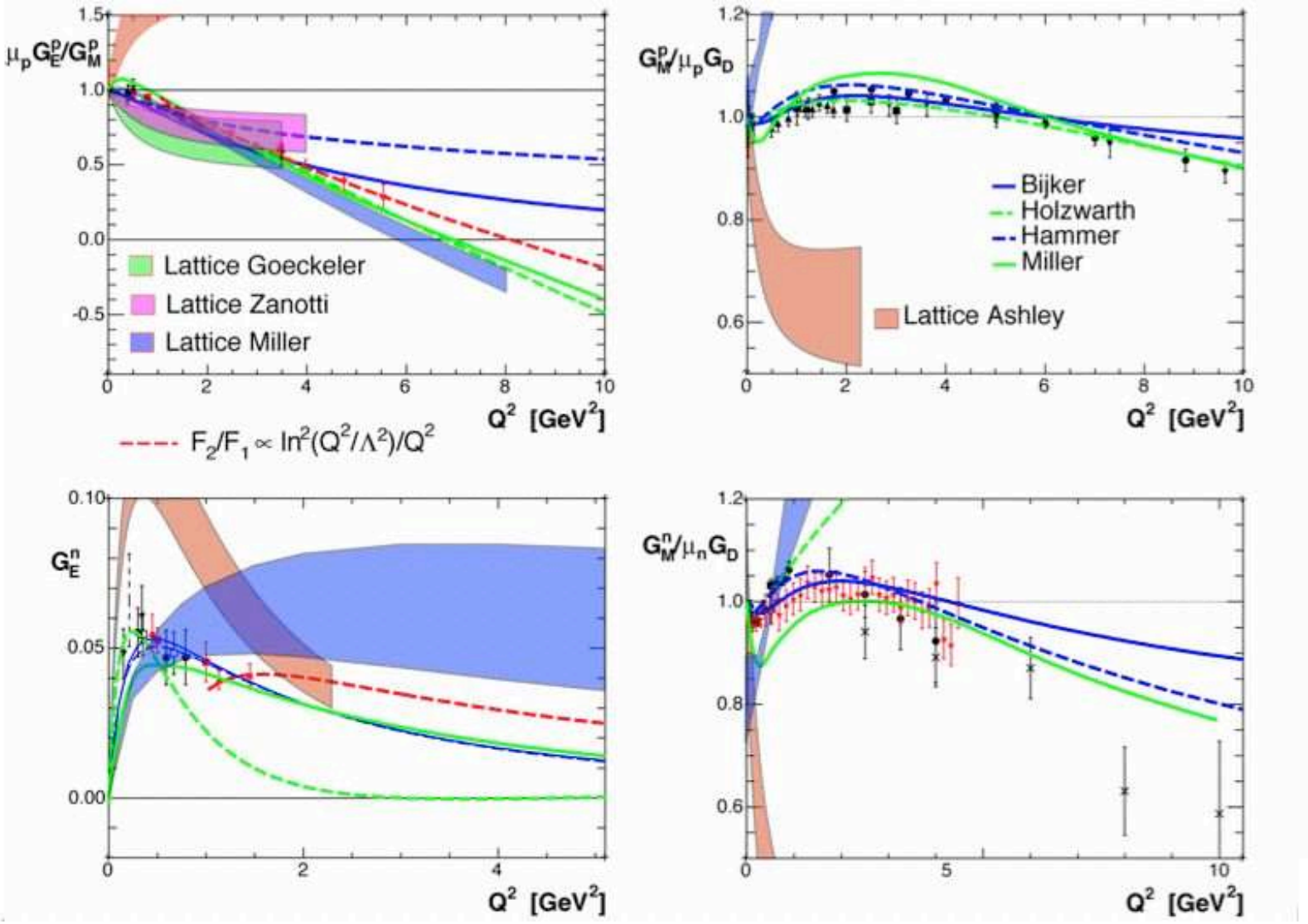

Planned measurements of G_E^p

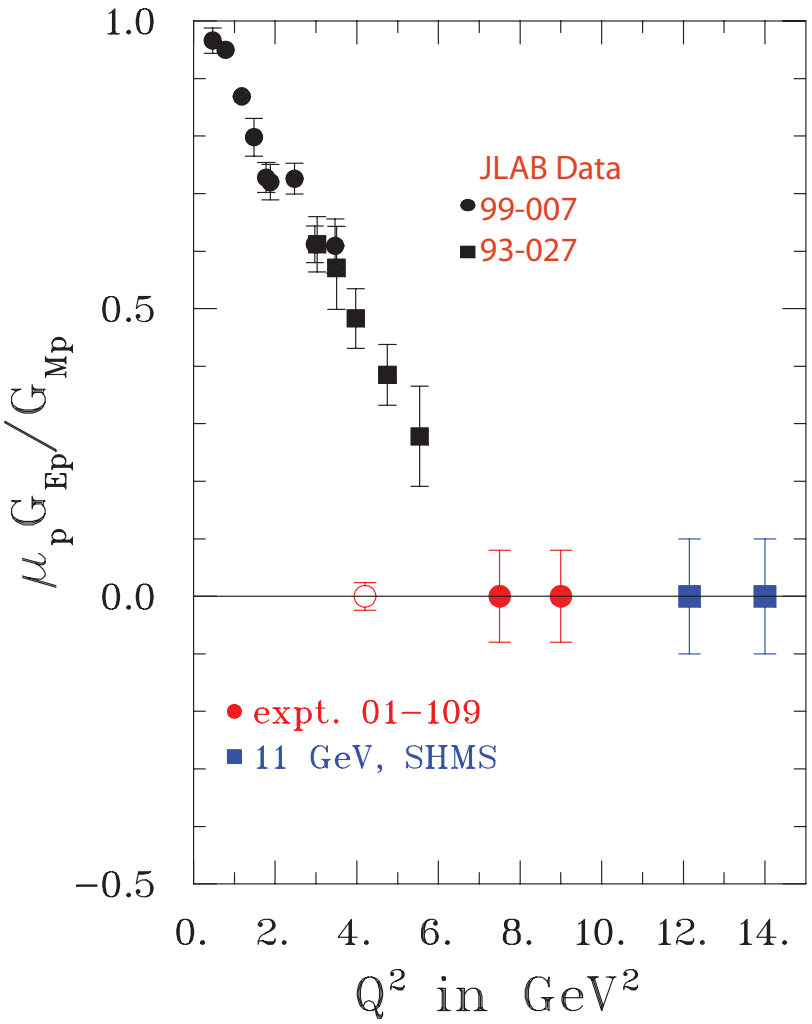

- Perdrisat *et al.* E01-109 (runs in late 2007)
- uses Hall C HMS (with new FPP) and BigCal
- SHMS in Hall C at 11 GeV (2013+)

More G_E^n

✷ G_E^n via $^3\overrightarrow{\mathrm{He}}(\vec{e}, e'n)$ out to $Q^2 = 3.4$ (GeV/c)^2 in Hall A at JLAB

Just completed!

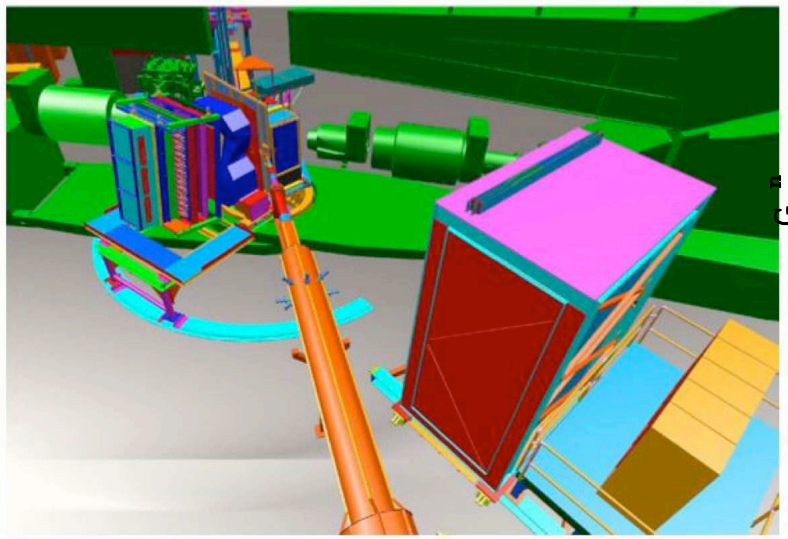

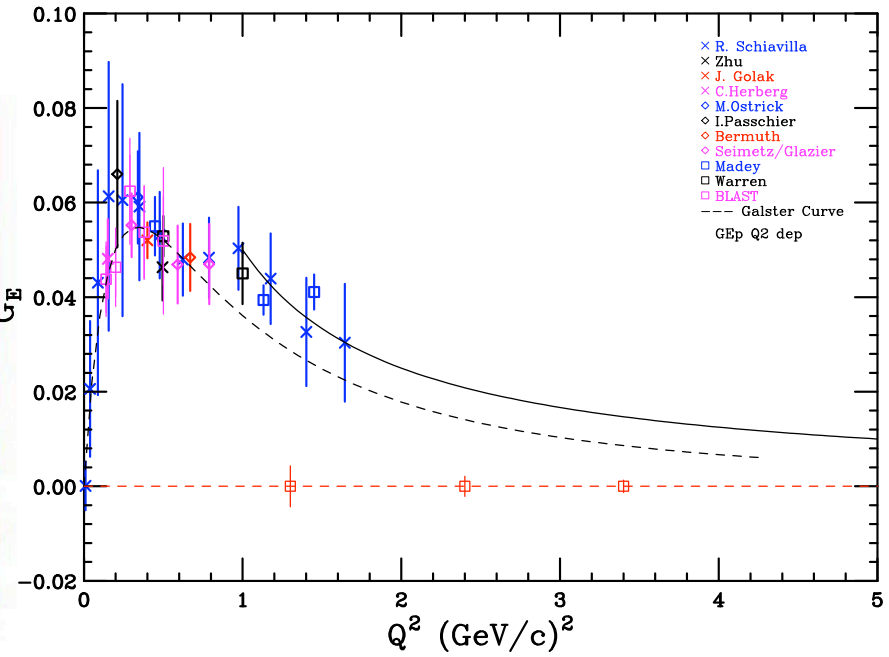

At 11 GeV increased acceptance and improvements to recoil polarimeter or ^{3}He target will allow measurements to $\simeq 8$ (GeV/c)^2

Prospects for future measurements

- Precision measurements of G_E^n out to $Q^2 = 1.5$ (GeV/c)^2 at Mami-C via $^3\overrightarrow{\mathrm{He}}(\vec{e}, e'n)$
- Precision measurements of G_E^p at Mainz, up to 1 (GeV/c)^2
- G_E^n via $^3\overrightarrow{\mathrm{He}}(\vec{e}, e'n)$ out to $Q^2 = 3.4$ (GeV/c)^2 in Hall A at JLAB

  Extension to 5 (GeV/c)^2 in Hall A with 12 GeV upgrade.
- G_E^n via $^2\mathrm{H}(\vec{e}, e'\vec{n})p$ to 4.5 (GeV/c)^2 at JLAB's Hall C
- Form factor ratio (G_E^p/G_M^p) out to 9 (GeV/c)^2 via $^1\mathrm{H}(\vec{e}, e'\vec{p})$ in Hall C at JLAB with 6 GeV beam, 2005-2006.
  - Extension out to 12.4 (GeV/c)^2 with 12 GeV upgrade.
- G_M^n out to 14 (GeV/c)^2 with an upgraded CLAS and 12 GeV upgrade.

Conclusion

- Outstanding data on G_E^p out to high momentum transfer – spawning a tremendous interest in the subject and the re-evaluation of our long held conception of the proton.
- Finally G_E^n measurements of very high quality from Bates, Mainz and Jefferson Lab out to 1.5 $(\mathrm{GeV/c})^2$ exists, allowing rigorous tests of theory.
- Data sets out to large Q^2 from future experiments will further constrain any model which attempts to describe the nucleon form factors.
- A resolution of the G_E^p data from recoil polarization and Rosenbluth techniques will have applications in similar experiments from nuclei and deepen our understanding of physics and experiment.

Although the major landmarks of this field of study are now clear, we are left with the feeling that much is yet to be learned about the nucleon by refining and extending both measurement and theory. *R.R. Wilson and J.S. Levinger, Annual Review of Nuclear Science, Vol. 14, 135 (1964).*

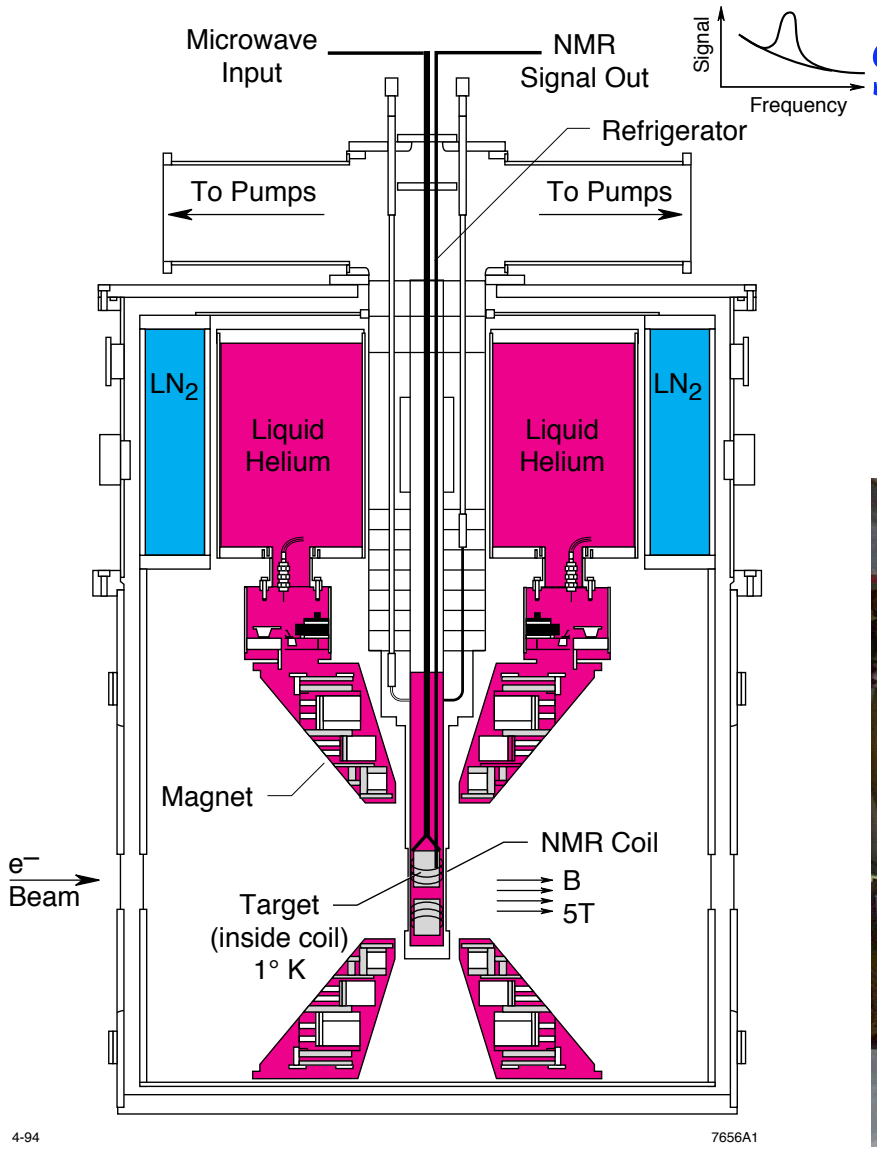

Solid Polarized Targets

- frozen(doped) $^{15}ND_3$
- ^{4}He evaporation refrigerator
- $5T$ polarizing field
- remotely movable insert
- dynamic nuclear polarization

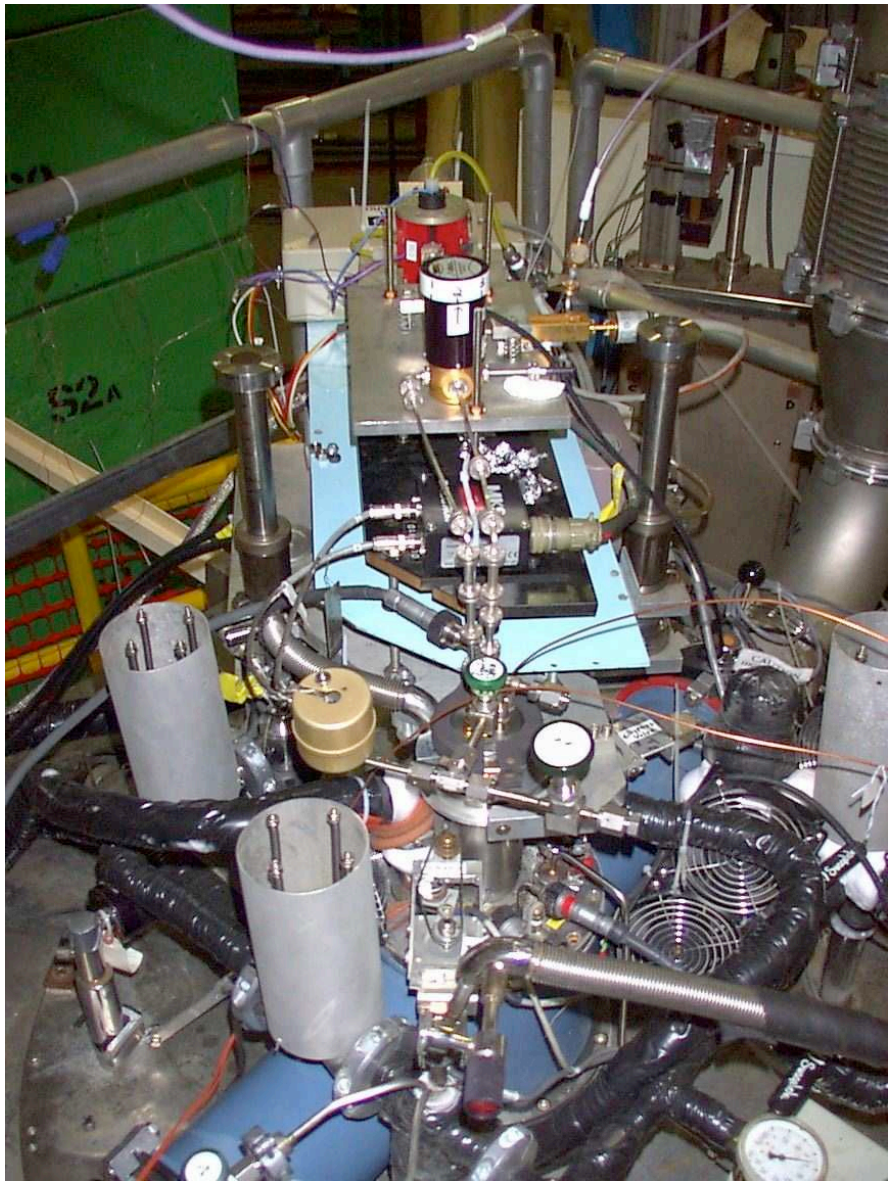

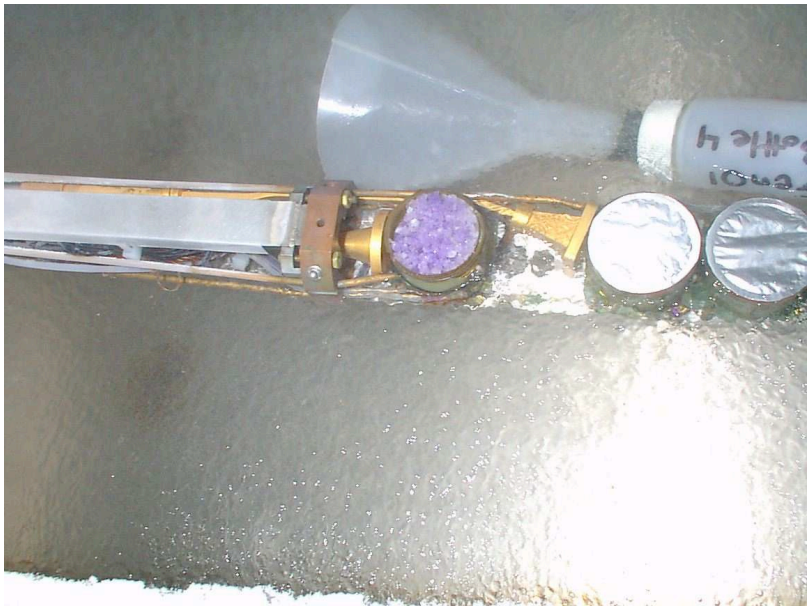

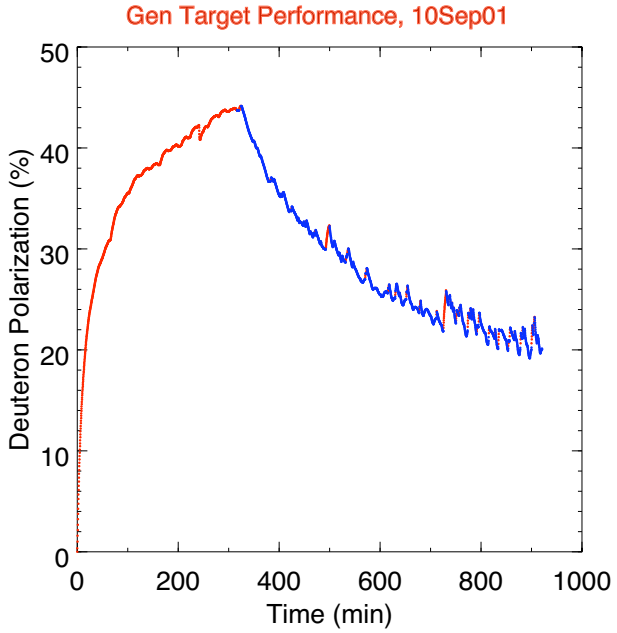
Gen Target Performance, 10Sep01
Deuteron Polarization (%)
Time (min)
0
10
20
30
40
50
0
200
400
600
800
1000